Chapter 4

CHEMISTRY CONTROL AND MONITORING SYSTEMS*

4.1 Introduction

The development of heavy liquid metal chemistry control and monitoring is one of the issues that is critical for nuclear systems using lead alloys either as a spallation target or as a coolant in the reactor primary circuit of a critical or sub-critical system, from the contamination control point of view as well as from the corrosion point of view.

Corrosion rates at temperatures below 450°C are rather low and satisfactory operation in this temperature range can be achieved using many materials including stainless steels and alloy steels. However, low temperature operation comes at a sacrifice of thermal efficiency, which will have a direct effect on the economics of plant operation for any power producing system. Thus, for applications where economic power generation is the goal, reduced temperature operation is not an acceptable solution. This is especially true for fast reactor systems where capital cost is generally considered higher than that for current light water reactor systems. In the case of ADS and other non-critical systems, however, operation at a temperature for which corrosion becomes acceptable is an option. Low temperature operation does not, however, eliminate the production of spallation and activation products or other contaminants, such as the oxygen or the corrosion products.

Then, for the operation of an HLM nuclear system, the chemistry control and monitoring is a critical issue for at least three distinct requirements:

1) Contamination, the assurance of stable hydrodynamics and heat transfer during service lifetime requires that PbO production be avoided. Lead oxide production may result in plugging due to mass transfer in a non-isothermal system. Also, deposits of other contaminants may eventually reduce the overall heat transfer capacity, etc.
2) Corrosion and/or dissolution must be kept to a minimum to ensure sufficient resistance of the structural materials during the expected service lifetime. This might require the use of active oxygen control to promote and maintain a protective film, although other method could be applied (see Chapter 6).
3) Activation due to corrosion, spallation and fission products might require liquid metal specific control to ensure safe management of the operation and maintenance phases.

The satisfaction of the above requirements makes chemistry control an essential element of nuclear system operation: control of oxygen and other relevant impurities including corrosion products, spallation and activation products. To this end, control processes, in conjunction with monitoring systems, must be developed and/or qualified for application to an ADS system for both the coolant loop (refereeing to the primary circuit), for the spallation target loop and for the primary circuit in any critical system. These issues will be discussed in detail in the following sections.

---

* *Chapter lead: Jean-Louis Courouau (CEA, France).*

4.2 Oxygen control in lead and LBE systems

The oxygen is clearly the most important chemical compound for any lead alloy system, because of its potential contamination rate, as well as because of its consequences on the contamination by solid oxides, and its main influence on the corrosion rate of iron-based structures [Shmatko, 2000] [Zrodnikov, 2003] [Martynov, 2003] (see also Chapter 6).

Oxygen comes from the start-up operations, from the maintenance phase as well as possibly from the incidental contamination, for which operating steps the oxygen saturation is more than likely [Courouau, 2003a, 2005a]. To the opposite, its contamination source should be negligible during normal operating mode. If the oxygen concentration must be adjusted to a specified value for corrosion control, the issue of implementing an oxygen contamination source arises. Contrarily, systems for oxygen purification would be necessary for the start up, restart, or maintenance phases. Therefore, the followings points that describe the requirements for operating a nuclear lead alloys system will be detailed hereafter:

1) the upper limit for oxygen to avoid the contamination by coolant oxides;
2) the lower limit for oxygen to enhance the corrosion protection by the self-healing oxide layer, which depends on the structure material – the iron-based alloy will be treated for illustration;
3) the oxygen control policy for nuclear operations, including the method to select the oxygen activity.

Finally, the issue of the homogeneity of the oxygen, which is present in very low concentrations in the lead alloys and submitted to various processes either consuming or releasing it, will be shortly discussed.

4.2.1 Upper limit for the oxygen for operational control

The coolant contamination by its oxides is defined by the solubility of oxygen in lead alloys, giving a maximum allowable oxygen chemical activity in the liquid metal. The following relations define theses limits for pure lead and LBE [Gromov, 1998] (see also Chapter 3), for which C_o^* stands for the dissolved oxygen concentration expressed in weight percentage:

$$\text{Lead: } \log C^*_{o(\text{wt.\%})} = 3.2 - \frac{5000}{T_{(K)}} \qquad \text{for } 400°\text{C} < \text{T} < 700°\text{C} \qquad (4.1)$$

$$\text{LBE: } \log C^*_{o(\text{wt.\%})} = 1.2 - \frac{3400}{T_{(K)}} \qquad \text{for } 400°\text{C} < \text{T} < 700°\text{C} \qquad (4.2)$$

The accuracy of these relations is not reported, especially for temperature lower than the specified temperature range, although this data is one of the key parameter of the lead alloys chemistry. It will have to be measured more accurately on a wider temperature range, as this relation is commonly extrapolated for the lower temperature. However, it is roughly confirmed by recent verifications [Ghetta, 2004] [Courouau, 2004a] [Ganesan, 2006] (see also Chapter 3).

The main oxide formed in liquid LBE is lead monoxide (PbO), as it is the most stable oxide when compared to other lead oxides and bismuth oxides [Gromov, 1998]. The upper oxygen chemical activity needed to avoid contamination is then defined by the lead monoxide solubility, although in case of a large oxygen contamination, both lead and bismuth oxides will be formed.

In order to calculate dissolved oxygen concentration, the hypothesis of an ideal solution is often made, and the Henry's law is applied to the dissolved oxygen. Assuming solid lead monoxide as the standard state for the oxygen in lead alloy, the oxygen activity, a_O, shall be equal to unity when saturation is reached [Borgstedt, 1987]:

$$a_O = \frac{C_o}{C_o^*} \tag{4.3}$$

where C_o is the dissolved oxygen concentration and C_o^* is the saturated oxygen concentration.

The operating specification to avoid any oxide precipitation in the coolant is then:

$$a_O \leq 1 \quad \text{or} \quad C_o \leq C_o^* \tag{4.4}$$

This specification must be ensured for all operating temperatures in any point of the loop, both in the liquid bulk as well as at the wall interface.

Table 4.2.1. Oxygen solubilities in lead alloys expressed in μg/g or ppm*

	130°C	200°C	330°C	400°C	500°C	600°C	700°C
Lead	–	–	0.08	0.6	5.4	30	115
LBE	0.0006	0.01	0.4	1.4	6.3	20	51

* Concentration expressed in weight percentage converts to μg/g (or ppm) by the multiplication by 10^4 or by addition of 4 in the log-type relation.

Table 4.2.1 presents some values for the oxygen solubilities in lead and lead-bismuth eutectic at relevant temperature for a nuclear system operation LBE using Eq. (4.1) and Eq. (4.2) LBE [Gromov, 1998]. As main operating consequence, the safety margin to avoid oxide precipitation is very limited, especially in low temperature range, and its potential risk of circuits clogging is then a real issue. Indeed, any small change in the coolant chemical conditions may induce very quickly oxide precipitation that is not acceptable for a nuclear system.

The upper limit for the oxygen that will be allowed in any non-isothermal system is generally defined by the point where oxide is formed first: the surface of the coldest point because of the thermal gradient between the wall and the liquid bulk, and because oxide can be formed there and thrown elsewhere in the circuits [Shmatko, 2000]. For illustration, if the minimum temperature of the surface of a LBE system is 200°C, the upper oxygen limit for operation would be 0.01 ppm.

4.2.2 Lower limit for the oxygen for operational control

Almost all of the elements of significance for structural material development have a lower equilibrium oxygen partial pressure than heavy liquid metal such as lead and bismuth for their oxides. It is then possible, from a theoretical point of view, to promote a protective oxide film by assuring that the oxygen potential in the liquid metal is above the potential for film formation on the structural material for use in the high temperature range (>450°C) (see also Chapter 6). This active oxygen control scheme for corrosion protection has been widely studied for steel structure by the formation of an iron-oxide film (magnetite, Fe_3O_4) [Gorynin, 1998]. Russian test data on steels in liquid lead alloy have shown that there exist three different yet distinctive corrosion regimes as function of oxygen concentration. When the oxygen concentration is too low for a stable oxide film, dissolution of metal

occurs. At high oxygen concentrations rapid oxidation occurs which results in degradation of the structure and/or the formation of Pb oxides. Between these two extremes, there exists a transition region where the kinetics transitions between dissolution and oxidation and the overall reaction rate is kept very small [Ballinger, 2004].

The reliance of an oxide film based on an alloying element of the structure require that the oxygen potential be controlled within a narrow band, the upper oxygen potential being defined by the contamination by Pb oxide, and the lower oxygen potential by the conditions of formation of the protective oxide. The following structural elements are foreseen for corrosion protection by the formation of oxide film, except iron: Cr, Zr, Si, Al [Ballinger, 2004]. ZrO_2, Al_2O_3, SiO_2 or SiC can be considered as low solubility materials or be used as barriers layers to limit the corrosion. From the viewpoint of active oxygen control, the lower oxygen limit is firstly determined by the relative thermodynamic stability of the oxide when compared to Pb oxide, the more stable the lower the oxygen potential, and the largest operational temperature range (see also Chapter 3).

First, the stability of various oxides is compared to each other thanks to their free energies of formation (Ellingham diagram). Reactions are written for the consumption of one mole of di-oxygen:

$$\frac{2x}{y} Me_{(dissolved)} + O_{2(dissolved)} \longrightarrow \frac{2}{y} Me_X O_Y \tag{4.5}$$

The unit is then expressed in J/mol of oxygen O_2. Calculation is made with HSC database software [HSC, V4.1], and the coefficients of the linear regression in the temperature range 400-1000 K, or 127-727°C, are computed to give the standard free enthalpies of formation in the useful operating range, and reported in Table 4.2.2. Indeed, the construction of ΔG – T diagram is useful to determine the relative areas of stability for one oxide, using the activities product of the previous reaction:

$$\Delta G = RT \cdot \ln P_{O_2} \text{ and } \Delta G^o = RT \cdot \ln P^o_{O_2} \tag{4.6}$$

All points of such a ΔG – T diagram are then meaningful:

- for $\Delta G > \Delta G^o$, the system is outside is equilibrium conditions, and only oxide is present;
- for $\Delta G = \Delta G^o$, the system follows its red-ox equilibrium, where both oxide and the metal are present;
- for $\Delta G < \Delta G^o$, the system is outside its equilibrium conditions, and no oxide is stable.

The corresponding ΔG – T diagram is plotted in Figure 4.2.1, presenting clearly the more stable and the least stable oxide from a thermodynamic point of view in liquid lead alloy. The isoconcentration lines of dissolved oxygen for respectively 0.01 and 10^{-10} ppm in weight in LBE melt are also plotted for comparison. In particular, it can be noticed that the window for an active oxygen control for corrosion protection by iron oxide film corresponds to the narrow: area delimited by the PbO line (below) and the Fe_3O_4 line (above). To the opposite, all other potential oxides for other structure candidate materials, SiO_2, Cr_2O_3, Al_2O_3, and ZrO_2 present oxides that will be stable over the whole range of oxygen potential in the liquid metal alloys, including in the higher temperature range.

Figure 4.2.1 is plotted with activity of all impurities equals to unity, meaning that all elements are dissolved in the LBE up to their solubility limit. This is unlikely to happen in nuclear system where impurities from the alloying elements of the structure as well as dissolved oxygen are submitted to mass transfer within the circuits, including release to the liquid metal by corrosion/dissolution of the

Table 4.2.2. Main oxides free enthalpies coefficients for the 400-1000 K temperature range, and for one mole of oxygen computed from [HSC v4.1] (see also Chapter 3)

$\Delta G^o = \Delta H^o - T.\Delta S^o$	ΔH^o (400-1000 K) kJ/mol	ΔS^o (400-1000 K) J/mol/K
4/3 Al + O_2 = 2/3 Al_2O_3	-1117.15	-209.8
4/3 Bi + O_2 = 2/3 Bi_2O_3	-389.14	-192.6
4/3 Cr + O_2 = 2/3 Cr_2O_3	-755.41	-171.8
4/3 Fe + O_2 = 2/3 Fe_2O_3	-544.13	-171.2
3/2 Fe + O_2 = 1/2 Fe_3O_4	-551.99	-156.9
2 Fe + O_2 = 2 FeO	-529.19	-131.4
2 H_2 + O_2 = 2 H_2O(g)	-490.31	-104.5
2 Ni + O_2 = 2 NiO	-473.69	-175.7
3/2 Pb + O_2 = 1/2 Pb_3O_4	-357.93	-192.1
2 Pb + O_2 = 2 PbO (litharge < 762 K)	-439.87	-198.8
2 Pb + O_2 = 2 PbO (massicot)	-437.61	-199.1
Pb + O_2 = PbO_2	-273.60	-195.5
Si + O_2 = SiO_2	-909.32	-179.6
Zr + O_2 = ZrO_2	-1094.54	-187.21

Figure 4.2.1. Ellingham diagram for lead-bismuth eutectic melt

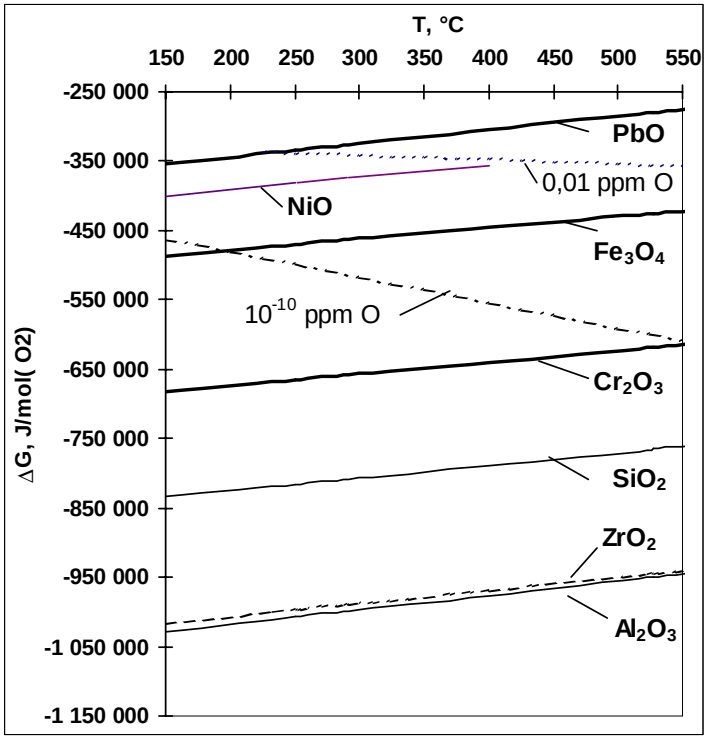

structure as well as precipitation/oxidation, so the actual activity results from a dynamic equilibrium, which may be very far from unity. Detailed analysis for the iron-based structure is given hereafter for illustration of the methodology used for specifying the lower limit for the oxygen for operational control.

Assuming iron-based alloys and corrosion protection by self-healing oxide layer, the oxygen potential must ensure the conditions for the formation of iron oxide in any part of the system, in the liquid bulk as well as at the wall interface, for all operating conditions. Indeed, the magnetite being the least stable oxide of the layer, it defines the minimum allowable oxygen concentration. The reaction of the steel oxidation in liquid lead alloys is assumed to be as follows:

$$\tfrac{3}{4}\,\mathrm{Fe}_{(\text{dissolved})} + \mathrm{PbO}_{(\text{dissolved})} \longrightarrow \tfrac{1}{4}\,\mathrm{Fe_3O_4} + \mathrm{Pb}_{(\text{liquid})} \tag{4.7}$$

where oxygen is supposed in solution in the form of dissolved PbO under its saturation limit. This is equivalent to consider that a cloud of Pb atoms surrounds the O atom. Dissolved oxygen chemical activity is then referring to dissolved PbO activity. Computed from Table 4.2.1 the standard free enthalpy of reaction is then:

$$\Delta_r G^{o}{}_{(\text{J/mol})} = -57190 - 21.1 \cdot T_{(K)} \tag{4.8}$$

Lead activity is equal to unity in pure lead solution, and is given by the following Russian relation in LBE solution as quoted in [Courouau, 2002b], which is slightly lower than 0.45:

$$\ln a_{\mathrm{Pb}} = -\frac{135.21}{T_{(\mathrm{K})}} - 0.8598 \tag{4.9}$$

The iron solubility in lead or lead alloys is expressed as [Gromov, 1998] [Tecdoc 1289], and illustrated in Table 4.2.3:

$$\text{Lead: } \log \mathrm{C}^{\mathrm{s}}_{\mathrm{Fe(wt.\%)}} = 0.34 - \frac{3450}{T_{(\mathrm{K})}} \qquad \text{for } 330°\mathrm{C} < \mathrm{T} < 910°\mathrm{C} \tag{4.10}$$

$$\text{LBE: } \log \mathrm{C}^{\mathrm{s}}_{\mathrm{Fe(wt.\%)}} = 2.01 - \frac{4380}{T_{(\mathrm{K})}} \qquad \text{for } 550°\mathrm{C} < \mathrm{T} < 780°\mathrm{C} \tag{4.11}$$

Table 4.2.3. Iron solubilities in pure lead and LBE expressed in μg/g (ppm)

	130°C	200°C	330°C	400°C	500°C	600°C	700°C
Lead		–	0.04	0.16	0.75	2.4	6.2
LBE	10^{-5}	0.0006	0.07	0.3	2.21	10	32

The activity product of the reaction of formation of magnetite in lead alloys is then as follows for equilibrium conditions:

$$\ln\left(a_O \cdot a^{3/4}{}_{\mathrm{Fe}}\right) = \ln a_{\mathrm{Pb}} + \frac{\Delta_r G^{o}}{RT} \tag{4.12}$$

Defining the iron activity similarly to the oxygen activity, $a_{\mathrm{Fe}} = C_{\mathrm{Fe}}/C^{*}_{\mathrm{Fe}}$, it is equal to one when the iron is saturated in the solution, and defining the minimum oxygen concentration required for effective corrosion protection, $C_{o\,\min}$ (in wt.%), the following relations are derived:

$$\text{Lead: } \log C_{O\min(\%)} = -\frac{3}{4}\log C_{Fe(\%)} + 2.355 - \frac{10600}{T_{(K)}} \tag{4.13}$$

$$\text{LBE: } \log C_{O\,min(\%)} = -\frac{3}{4}\log C_{Fe(\%)} + 1.2375 - \frac{9757}{T_{(K)}} \tag{4.14}$$

If the system enters the dissolution area, and if *in situ* oxide layers protect the structure, there will be a certain time lag corresponding to the time required to dissolve the magnetite and spinel oxide layers. This somehow introduces a safety margin. Conversely, when going back to the right oxygen level, there will be some delay. During these periods, the only measurement of oxygen is not enough, as oxygen concentration will be kept stable, defined by the iron oxide chemical reaction equilibrium. This is analogous to a buffer effect. The only way to detect if the oxide layer is dissolving or growing would be to measure directly its thickness using an electrical resistance probe measurement [Provorov, 2003].

The lower limit for the oxygen that will be allowed in any non-isothermal system is generally defined by the point where the iron oxide will be dissolved first: the surface of the hottest point because of the thermal gradient between the wall and the liquid bulk. For illustration, if the maximum temperature of the surface of a LBE system operating with a structure made of iron based alloy is 650°C (hot spots), the lower oxygen limit for ensuring the iron oxide formation would be about 0.0005 ppm.

4.2.3 Specifications for active oxygen control

The oxygen concentration areas of operation to ensure both no contamination, required for any system, and possibly corrosion protection for higher operating temperature are similar for the liquid lead or the lead-bismuth eutectic:

$$C_{o\,min} \leq C_o \leq C_o^* \tag{4.15}$$

The operating specifications for oxygen is evaluated from the Figure 4.2.2 drawn with the previous relations illustrated for active control for iron-based structure, knowing that for other non-ferrous structure materials, the specification for active oxygen control for corrosion protection would be less restrictive.

The minimum oxygen concentration required to ensure the oxide layer stability is plotted against the saturated iron content, which maximises the oxidation area as for lower iron concentration the minimum oxygen concentration increases (Figure 4.2.2) [Gromov, 1998] [Shmatko, 2000]. For an isothermal system, a vertical line plotted at the system temperature defines the oxygen range that is allowed: as illustrated in Figure 4.2.2, a system operating at 420°C is giving an oxygen range of $2.5\ 10^{-6}$ to 2 wt-ppm. In principle, for a non-isothermal system, the intersection of the two ranges defined by the vertical lines plotted respectively for the cold and the hot legs temperatures are defining the oxygen range. As illustrated in Figure 4.2.2, a system operating between 420°C and 540°C would then give an oxygen range of $6\ 10^{-5}$ to 2 wt-ppm.

For non-isothermal systems, the temperature at the interface is different from the bulk temperature because of the heat transfer process. However, if the oxide layer protection is required, the minimum oxygen content must be ensured at the wall temperature, which defines the oxygen concentration range allowed for operation for a given system. For instance, in the BREST-300 like coolant, the

operating conditions are: operating coolant temperature 420-540°C, maximum fuel clad temperature of 650°C (hot spots), and minimum steam generator wall temperature of 200°C [Shmatko, 2000]. Thus, the oxygen concentration must be kept lower than 0.01 wt-ppm to prevent coolant oxidation at 200°C and higher than 0.0005 wt-ppm to keep oxide protection at 650°C for saturated iron activity ($a_{Fe} = 1$), that could be compared to the range defined only by the bulk temperatures: 6 10^{-5} wt-ppm (420°C) to 2 wt-ppm (540°C) which is drastically larger. If the same kind of conditions are required for lead coolant, the range of oxygen to ensure no contamination and corrosion protection by iron oxide is 0.31 wt-ppm at 375°C and 2.6 10^{-3} wt-ppm at 650°C, which is even narrower [Courouau, 2004b].

Figure 4.2.2. Oxygen specifications in LBE

For a BREST-300 like primary coolant, showing in shaded area the allowable oxygen operating range, as well as the contamination ($C_o=C_o^*$), the oxidation ($C_{omin} < C_o < C_o^*$) and the dissolution ($C_o < C_{omin}$) areas

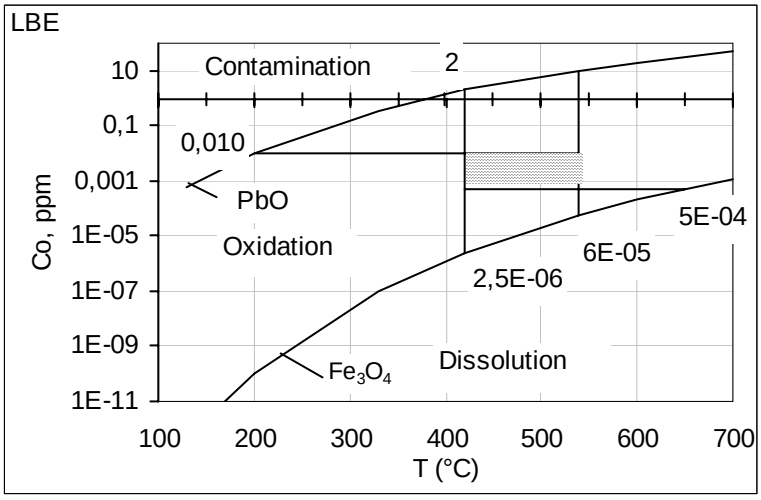

However, the condition that iron is present in saturated condition is foreseeable in static condition, but unlikely in dynamic loop condition where mass transfer will play a role. Indeed, in a non-isothermal system, the iron will be released from the hot structural wall by corrosion, and transferred to locations with lower temperature, where it may precipitate. The diffusion and the convection processes are the 2 mechanisms responsible for the mass transfer: usually, the diffusion of the species from the wall to the liquid bulk through the boundary layer is the limiting process. This latter includes the diffusion through the oxide layer when it is present. The thermodynamic condition for oxide formation on the interface can then be quite different from the condition in the liquid bulk, which is the result of a dynamic equilibrium ($a_{Fe} < 1$). Figure 4.2.3 illustrates this: decreasing the iron concentration reduces the oxidation area, the higher the temperature the higher the reduction. For working at higher temperature, the oxygen content should then be close to its saturation limit. Indeed, the iron in equilibrium with its oxide at the wall interface can then be several orders of magnitude lower than its solubility, which reduces in turn the corrosion rate to low or very low level. This is the working mechanism behind the active oxygen control and the oxide film formation [Gromov, 1998] [Shmatko, 2000] [Li, 2002], which was recently more fully investigated from a theoretical point of view [Martinelli, 2005].

It can be noticed that the higher the operating temperature and the smaller the oxidation area, which will eventually prevent the use of active oxygen control for corrosion control by iron oxide film formation in the high operating temperature range (around 700°C).

Figure 4.2.3. Iron oxide formation threshold defining the couple of solution to ensure a protective oxide layer depending on both the iron (C_{Fe} or c) and oxygen concentrations (C_o), in LBE expressed in wt.% and ppm respectively for the left and the right hand side graph

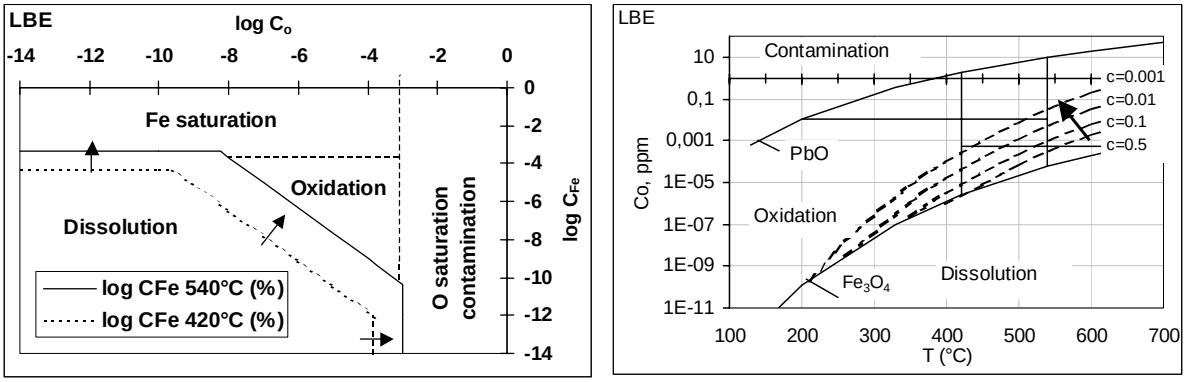

The iron concentration is difficult to measure and impossible to monitor on-line up to now. The lower detection limit is 5 wt-ppm by chemical analysis up to now, and could possibly be lowered to 0.5 wt-ppm, which may still be higher than the iron concentration expected. There is no straight solution to control the iron content, but oxygen should be controlled and monitored on-line so that it gives at least the hand on one parameter. As a consequence, the oxygen specification should be set at the highest possible value that complies with the contamination requirement, which corresponds to the cold leg temperature interface, as this is maximising the oxidation area for an unknown iron concentration, which is defining the specification for oxygen control:

$$C_o\left(\text{Contamination} \middle/ \text{and corrosion} \quad \text{control}\right) = C_o^*\left(\text{cold leg wall temperature}\right) \tag{4.16}$$

From the previous example, the oxygen concentration specification chosen would then be 0.01 wt-ppm.

This thermodynamic analysis was made thanks to some assumptions, and could be more or less well applied to perlite steel (Fe 100%), but might be slightly different for Cr alloyed steel or even, Zr, Si, or Al based materials or corrosion barrier materials, as the oxide layer will be a compound of more stables oxides. Real operating limits should be measured on test facilities in representative operating conditions and for relevant materials.

4.2.4 Policy for a nuclear system

The oxygen control is then a basic requirement for nuclear relevant system, for which long service lifetime is expected, meaning interventions for components and fuel handling, repair and maintenance, requiring a purification of the oxygen before any restart, together with a requirement for a as high as possible operating temperature, which might require the corrosion control by self-healing oxides layer on the structural iron-based materials.

The contamination represents the main issue during the initial operations (first filling, start-up…) [Ivanov, 2003a] [Courouau, 2004c, 2005a], as well as during the maintenance and repair phases: air ingress can happen and the oxygen is released from the structural materials as well as from the LBE itself. It is critical to ensure that the liquid metal is kept clean and that no solid oxides are formed, as

these could possibly clog narrow sections of the facility, or deposit on heat exchanger surface, so that the overall cooling capacity of the system can be affected. However, it is reported [Martynov, 2005], and usually well observed, that there are no difficulties during the start-up of facilities from the viewpoint of the coolant purity and cleanliness, meaning that a few percent of solid lead oxide in the liquid metal melt appears still compatible with flowing conditions. However, the accumulation the long-term operation of the oxide, if not treated regularly, will eventually hinder the operation of the facilities by affecting its cooling capacity (clogging, deposits on pipes). Amount of solid oxide and deposit in circuits were recorded up to 5% of the coolant mass in the circuit [Martynov, 2005]. These deposits are composed of mainly PbO and LBE, with traces of iron, and are not affected by high temperature or by low oxygen concentration. Such occurrence of a two-phase flow is not acceptable for nuclear operation, so that the contamination must first be reduced to the minimum, as well as systems for regular purification must be implemented [Martynov, 2005].

Known major oxide slag formation failures date back from the 60s: the initial run of the KV/27 land nuclear reactor based at IPPE and the project 645 nuclear submarine failure on cruise [Ivanov, 2003b]. For the latter, a sudden ingress of slag in the core during sea trials in 1968 caused a loss of power by negative temperature reactivity effect. The crew tried to restore the power by levelling off the control rods that led to partial melting of the core. In fact, there were at least two sources of contamination for the coolant: the oxygen accumulated during the maintenance phases and the oil contamination from the rotating shaft of the primary pumps. As there were no quality-monitoring devices, nor process for purification, the slow ongoing contamination and accumulation could not be detected nor treated, eventually leading the nuclear failure of the system.

By contrast, during the normal operating mode, the oxygen contamination sources are then negligible, so that, because of the various source of consumption of the oxygen, one can expect low or very low oxygen content in the liquid metal loop [Shmatko, 2000]. The corrosion control by active oxygen control could then be critical during that operating period, depending on the choice of the materials, and of the operating temperatures. For iron-based alloys and for temperature higher than 450°C, for which the corrosion rates by dissolution become nor more negligible, the active oxygen control would be required. The use of other materials, such as low solubility materials such as composite SiC, ceramic Al_2O_3, ZrO_2 that presents low solubility in lead alloys, or applied on a substrate materials as a barriers layers [Ballinger, 2004], may present a so large area of use as regard the oxygen that the lower oxygen limit may not be achievable in practice, excluding any requirement for active oxygen control.

The requirements for oxygen control systems could then be divided into:

1) purification from oxygen during start-up, or restart to prevent the formation of lead monoxide;
2) active oxygen control for corrosion protection during the normal operating mode, and possibly at the initial stage to promote the formation of a protective oxide layer.

The first requirement consists in ensuring the contamination control in any part of the circuit and for any operating condition, in order to avoid the oxides formation of firstly the coolant oxides. This requirement is common to all nuclear systems.

The second requirement consists in active oxygen control for promoting a protective oxide film formation on the structure by controlling the oxygen potential in the liquid metal. This requirement depends on the design specifications of the systems, and firstly its operating temperatures, and then on the choice of the materials.

If no corrosion control is required, the contamination specifies the upper threshold for the oxygen control as follows:

$$C_o\left(\text{ontamination control only}\right) \le C_o^*\left(\text{cold leg wall temperature}\right) \tag{4.17}$$

This choice was made for the MEGAPIE target, thanks to the choice of low operating temperature (<400°C peaks) for the short service lifetime (6 months). Figure 4.2.4 represents the expected oxygen concentration during its service lifetime, from its start-up tests to the on-beam operations. Its service lifetime was assessed as compliant with the corrosion by dissolution of the steel at the low operating temperature chosen. However, Figure 4.2.4 clearly indicates that the conditions for dissolution would be achieved after a certain delay, necessary for the residual oxygen present in the liquid bulk as well as the residual oxide layer present on the steels to dissolve, which may takes weeks or months depending on the initial oxide layer and the production of hydrogen and spallation products. This time lag will limit the overall corrosion further on.

Figure 4.2.4. Oxygen expected behaviour for the MEGAPIE target during start-up operation (integral test stand – MITS), and during beam steady state operation where the oxygen will be reduced first down to the iron oxide stability threshold, and then even further down when all iron oxide will be reduced after an certain delay [Courouau, 2005a]

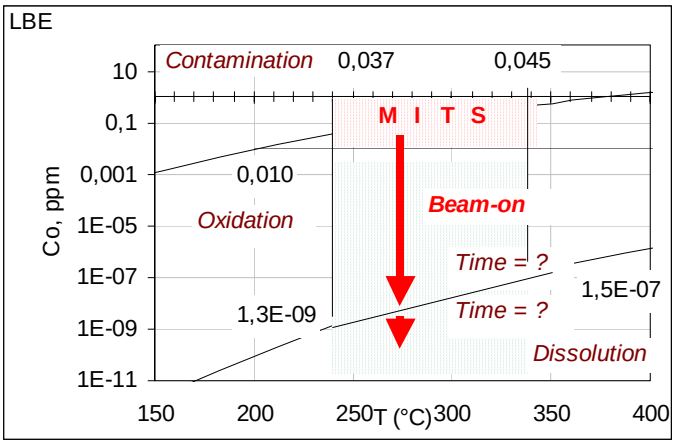

4.2.5 Oxygen control systems

The first requirement consists in ensuring the contamination control in any part of the circuit and for any operating condition, in order to avoid the oxides formation of firstly the coolant oxides. This requirement is common to all nuclear systems.

For any nuclear lead alloys circuits, it is necessary to provide the following systems for the oxygen control:

- oxygen measurement systems for on-line monitoring for the cover gas and the liquid metal;
- oxygen control systems for purification, and possibly for active oxygen control.

Indeed, the oxygen will behave accordingly between the cover gas and the liquid phase in normal operating condition, where equilibrium will be reached most certainly. As the main contamination sources are not part of normal operation, it is important to be able to detect the transient due to

contamination as soon as possible. As the transient could be very different from one phase to another, because of the large difference in volume, the oxygen measurement in both media is required. This was the main lesson learnt from the 1990 air contamination at SUPERPHENIX, where only liquid metal quality sensor was implemented, although the plugging-meters were actually indicating the occurrence of the contamination, but the correct interpretation was not done. Since then on, as it was already performed on PHENIX since the beginning, gas chromatography of the cover gas allows detecting any variation of nitrogen content that will allow detecting any air ingress quickly, as the oxygen reacts quickly with sodium.

The oxygen monitoring system for the liquid metal bulk, also referred to as the oxygen sensor, is part of a complete development in itself and will be detailed hereafter in a specific section. Measuring devices for the oxygen in the gas phase are commercially available.

The oxygen control processes will be briefly detailed hereafter.

Processes for the oxygen control in lead-bismuth systems are basically of two different kinds:

- gas phase control;
- solid phase control.

The principle of the gas phase control is based on gas/liquid equilibrium between the cover gas and the liquid bulk when the liquid is below saturation. Controlling the oxygen partial pressure in the gas phase would set the dissolved oxygen content.

In practice, pure oxygen or hydrogen are flowed in the cover gas, usually in dilution with argon, which is easy to achieve over flowing liquid in vessel, provided the interface is well mixed, or directly with the help of a bubbling line for a larger exchange area, in order to oxidise or reduce the liquid lead alloys according to the following reactions:

$$Pb_{(liquid)} + O_{2(gas)} \Leftrightarrow \quad PbO_{(dissolved)} \tag{4.18}$$

$$PbO_{(dissolved)} + \quad H_{2(Gas)} \Leftrightarrow H_2O \; + \; Pb_{(liquid)} \tag{4.19}$$

The use of hydrogen gas allows recovering from oxides accumulation after a large contamination, for star-up or maintenance, or after prolonged operations in order to restore the thermal-hydraulic performances of the system. The mechanical impact of bubbles is reported to increase the efficiency of the process by putting back into solutions particles of deposit, which should be used together with a filtration system [Papovyants, 1998]. The use of getter addition, such as Zr, or Mg, will reduce the oxygen to the low concentration but will produce other solid oxides at the same time that would have to be purified somehow. Hydrogen presents the main advantages to produce only a gaseous reaction product that is easily evacuated in practice through the vent line.

However, it is not easy to achieve the very low oxygen potential that is required for active oxygen control in the cover gas, so that the use of a ternary gaseous mixture is more practicable. Indeed, by fixing the ratio of steam over hydrogen for instance, the oxygen potential in the liquid metal is determined by the thermodynamic equilibrium [Gulevski, 1998], [Mueller, 2000], [Shmatko, 2000]. In principle, the use of other reaction system could be used, such as the CO/CO_2 system, but are not favoured for practical and safety reason. This can be used for the purification processes of system where oxide film is protecting the structure, in order to protect the oxide film from dissolution [Martynov, 2005]. Moreover, the use of a CO/CO_2 system should be evaluated with a special focus on the potential carburisation effects on the structural material.

The process parameters of the gaseous systems are related to the mass exchange at the gas-liquid interface that limits the equilibrium process in practice. Bubbling, which increases the exchange area greatly, favours the exchange, and then the time to reach the thermodynamic equilibrium. Temperature is the second main parameter for the hydrogen reduction of solid lead oxide [Ricapito, 2002], the higher the better, which might be related to the solubility. To the opposite, the oxidation is fast, which may lead to solid oxide formation rather than dissolved oxygen, which can be transferred and settled in other part of the facility, and then requiring subsequent purification. This is why oxidation at a slower rate is better achieved when adjusting directly the gas phase composition with the help of a ternary gas mixture.

To avoid the oxidation in excess and the solid oxide formation within the system, solid mass exchange was proposed [Gromov, 1996], [Zrodnikov, 2003]. It consists in dissolving solid lead oxide, which physical form is mechanically stable such as in pellet (Figure 4.2.5), in a device where the thermal-hydraulics is controlled. Indeed, the dissolution rate is depending on temperature and flow rate [Askhadulline, 2003, 2005], [Simakov, 2003], which give rise for the automated control of the oxygen by adjusting the consumption due to the oxidation with the contamination rate delivered to the system. The solid mass exchanger unit can be designed as a consumable item or for the whole service lifetime of small device such as spallation target, avoiding the handling requirement. Such a system will spare the needs for a complex gas circuits to be operated in a nuclear environment, except probably a regular venting out of the spallation residues, thus enhancing the confinement and the overall safety of the system.

Figure 4.2.5. Lead monoxide pellets device for oxygen supply to the coolant using the solid phase method [Martynov, 2003], [Askhadulline, 2005]

(G – liquid flow rate)

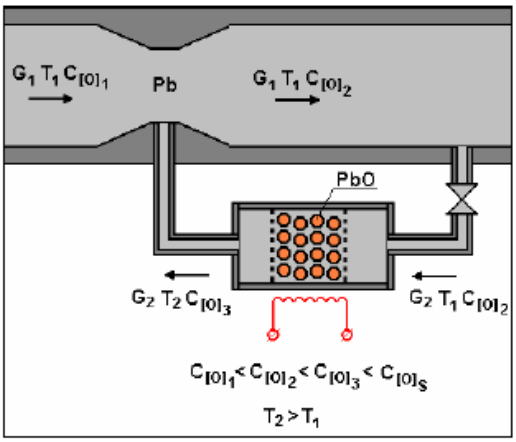

4.2.6 The oxygen homogeneity issue

Considering the oxygen as perfectly homogenised within the circuit [Shmatko, 2000], [Orlov 2005], i.e. that there is no limitation to the mass transfer because of the little convection/diffusion rate of the dissolved oxygen within the liquid metal, the oxygen concentration would be constant over the whole system. However, the condition for oxygen homogeneity is questionable. In the case of the corrosion protection, the oxygen range will be rather low, so that the process will only be qualified if the oxygen behaviour is controlled over all part of the circuits for all operating conditions. This means no lower oxygen spots where corrosion could happen, nor higher oxygen spots where Pb oxide can built up. This depends on the various convection and diffusion data for oxygen in lead alloys system (see also

Chapter 3), which are known as rather limited [Zrodnikov, 2003]. However, the low oxygen diffusivity in lead alloys could be, somehow, compensated for by higher convection in the system, ensuring the vigorous stirring of the liquid metal, and then its homogeneity.

In small scale systems, such as SVBR-75 [Toshinsky, 2000] or the Angstrem concepts [Tecdoc 1056], the liquid is renewed hundreds of times per hours, as illustrated in Table 4.2.4, so that the liquid phase can be assumed as perfectly stirred and homogeneous. In addition, as the volume of the coolant is small, there should be no stagnation zones. However, the highest flow velocity does not exceed 2 m/s on the fuel-cladding walls. For larger system the homogeneity might not be ensured, especially because of the lower convection. For instance, the pool-type liquid metal reactors, such as BREST or sodium-cooled reactors, the system mass change rates are 10 times lower than for the small-scale reactors (Table 4.2.4), primarily because these reactors hold considerably larger coolant volume. Dealing with the system mass change rate, the circulation loop-type reactor, when compared to pool-type, would be more efficient from the homogeneity point of view. Even though it would be necessary to compare in much more details distribution of Reynolds number in various parts of the reactors. The main event that can modify the distribution of impurities throughout the reactor (loop or pool type) is the shutdown or isothermal stand-by, which may affect the impurity distribution between hot plenum and cold plenum.

Table 4.2.4. Typical design parameters for core coolant circulation for various reactors

	Core flow rate	**Primary coolant**	**System mass change rate**	**Temperature**
PHENIX – 350 MWe (Na)	10260 t/h (3 * 0.95 t/s)	840 t	12 times/h	400-550°C (150°C)
SUPERPHENIX – 1500 MWe (Na)	61056 t/h (4 * 4.24 t/s)	3250 t	19 times/h	395-545°C (150°C)
EFR – 1470 MWe (Na)	61170 t/h	2100 t	29 times/h	395-545°C (150°C)
PWR – 1300 MWe (light water)	68000 t/h	380 m^3	179 times/h	286-323°C (37°C)
SVBR – 75 MWe (EPB)	3492 m_3/h (11.18 t/s)	18 m^3	194 times/h	275-439°C (164°C)
NPHP Angstrem – 30 t (EPB)	382 m3/h	3 m^3	127 times/h	280-465°C (185°C)
BREST – 300 MWe (Pb)	143640 t/h (3.8 m^3/s)	600 m^3 (6300 t)	23 times/h	420-540°C (120°C)
BREST – 1200 MWe (Pb)	570240 t/h (158.4 t/s)	2500 m^3 (26250 t)	22 times/h	420-540°C (120°C)

The recommendation from [Shmatko, 2000] is to provide at the circuit design stage provisions to avoid any perturbation of the flow (junction, abrupt turns, etc.), and to exclude any stagnation zones. This would in principle limit the contamination, accumulation, and potential rapid release due to thermo-hydraulic instability such as during hot stand-by and shutdown of the reactor.

However, the only possibility to validate a design for the safety authorities as regards the corrosion protection by self-healing oxide would be to model the mass transfer within the system, using accurate data on convection and diffusion of impurities, and appropriate relation to represent the corrosion/ precipitation phenomena in circuits [Zrodnikov, 2003], [Balbaud, 2001], [Li, 2002].

4.3 Characterisation of impurities and requirements for control

4.3.1 Impurity sources

One of the main, and most important, impurities is oxygen. However, there are other sources of contamination that could present some macroscopic effects on the operation even though occurring at a microscopic rate.

Apart from oxygen, the other main contamination sources include: (1) corrosion products (Fe mainly, Ni, Cr, etc.) expected to be generated continuously at a rate depending on the operating temperature, liquid metal flow rate, etc., (2) activation products from spallation, corrosion product activation, or fission (Po, Hg, Tl, Cs, Mn, ...) and (3) light particle production such as hydrogen (including tritium) within the reactor core, the sub-critical assembly or the spallation target.

In addition, if a self healing iron oxide film corrosion protection method is applied for iron based alloys, the oxygen must be controlled within a very narrow range, above the Fe_3O_4 formation potential but below the PbO formation potential (see Section 4.2.3). Advanced alloy systems that rely on either Si or Al based oxide formation for protection will expand the acceptable oxygen potential range. However, the effect of impurities, whether from the corrosion process itself, or due to contaminants introduced by other means can have a significant effect on the oxygen level required for protection, especially during transient phenomena, such as reactor hot or cold shutdown, which may affect dramatically the impurity distribution and stability within the liquid metal system. For this reason it is important that a complete determination of the potential impurities/contaminants be identified and characterised.

The sources of impurities can be listed by analysing the reactor system conditions during various operating modes including: (1) initial start-up before the first irradiation, (2) normal operating conditions, including start-up and shutdown; and, (3) transient & accidental conditions. Table 4.3.1 gives a synthesis of the various contamination sources expected for an accelerator driven system [Tecdoc 687&1289] [Courouau, 2003a, 2004b].

During normal operation, the only sources of contamination for an ADS system (primary circuit) will then be hydrogen and transition metal or metalloid impurities coming either from corrosion in the whole circuit or from spallation reactions in the target. An additional and incidental source of radio-contamination of a critical system would be from any failed fuel cladding.

A potential source of hydrogen in the intermediate circuits comes from the permeation from the steam generator units, if the energy conversion is performed with a Rankine cycle with steam, because of the steel aqueous corrosion as well as the thermal decomposition of the hydrazine (N_2H_4) added (in excess to the dissolved oxygen) in the water/steam circuits for reducing the aqueous corrosion. Actual diffusion rate will depend on the hydrogen partial pressure difference as well as on the oxide film thickness at the liquid lead alloys interface, of the steam-generator unit.

Another source of residual hydrogen would be from the proton beam in the spallation target and light element production by ternary fission that includes tritium. It can also be mentioned the degassing of hydrogen adsorbed during some fuel elaboration process, which is almost negligible.

For an ADS system, protons from the beam itself represent an intrinsic hydrogen source, as not all the protons injected into the system will result in a spallation reaction: unused protons will be thermalised and dissolved into the liquid metal as ionic hydrogen. The residual amount of hydrogen is however not well known. Spallation reactions generate hydrogen as well, in quantities that have been roughly assessed for instance for the MEGAPIE experiment to several litres of hydrogen, including

about 10% of tritium (69 l of LBE, 200 days of irradiation, 1.74 mA), which order of magnitude is not negligible, especially since the amount is steadily increasing with the irradiation time that could give rise to an accumulation effect in the spallation target, event though part of it reacts with oxides films or adsorbed gases.

Table 4.3.1. Typical impurities sources in nuclear HLM systems

A = coolant system of a critical or sub-critical reactor system, B = spallation target of an ADS

	Pollutions sources	A	B	Species	Impact
Normal operating conditions	Cover gas renewal	x	x	O; H_2O	Negligible
	Steam leak from SG	x		H_2O, (O, H)	Major if microleak or tube rupture
	Spallation residues, ternary fission and proton beam	x	x	H, tritium	Release to the environment
			x	Po, Hg, Tl, Au, Os and Ir	Release in case of loss of confinement
	Fuel/fuel cladding	x		^{54}Mn, ^{51}Cr, ^{59}Ni, ^{58}Co, ^{60}Co, ^{110m}Ag-110m	Coolant activation
	Corrosion products	x	x	Fe, Cr, Ni	Plugging/deposits
Initial start-up, restart after maintenance or repair	Dissolved oxygen	x	x	O	Plugging/deposits
	Intrinsic pollution	x	x	Ag, Cu, Sn, ..	Grade definition
	Gas adsorption in structures during maintenance	x		O; H_2O	Plugging/deposits
	Air inlet	x		O; H_2O	Plugging/deposits
Off-normal pollution sources	Fuel cladding failure	x		^{239}Pu, ^{235}U; ^{85}Kr, minor actinides and Cs, I, Kr, Xe nuclides	Activation on the long term
	Air ingress	x	x	O; H_2O	Plugging/deposits
	Steam ingress	x		H_2O	Cover gas pressurisation, plugging/deposits
	Casual pollution (oil, Hg, …)	x		Oil, Hg, Pb-Sn, …	Plugging/deposits

The ternary fissions have to be accounted for, as it is usually not negligible. Production depends from the ternary fission yields for ^{239}Pu, ^{235}U and ^{238}U. This produces all of the hydrogen nuclides continuously but at low rates, which is usually not negligible for the tritium with regards to the contamination release issue. As this impurity is produced inside the fuel rod, diffusion toward liquid metal is function of the fuel-cladding material, its operating temperature, and of the surface state of the material in contact with the liquid metal: steel retains almost no hydrogen or tritium, whereas zirconium alloys retains all hydrogen. Real transfer rate would have to be assessed for HLM systems, especially if specific coating (alumina) or surface modification treatment (GESA) is used, as it can significantly reduce the share of the contamination effectively transferred to the liquid media. In addition, if the use of neutron absorbers such as boron carbide is foreseen, its contribution to the tritium source would have to be accounted for, as its share might not be negligible when compared to the ternary fission contribution [Courouau, 2003a].

The steam generator units, if any, are normally designed as leak proof. However, some micro leaks could be expected, either because of the lower detection limit of the leak detection system, or because of some tolerance agreed for operation (a few litres/hours). From the liquid sodium reactor experience, a null leak rate between water-steam circuit and the secondary sodium circuit is, however, achievable, with extra constraints on the nuclear operation for the leak detection system and steam generator design. From the Russian experience [Toshinsky, 2000] [Shmatko, 2000], operation with small leaks is reported for some time without significant deviation of the designed technological parameters, which allowed the repair to be done at a convenient time. Indeed, the actual rate of oxidation in case of a small steam leak appears as limited [Shmatko, 2000] and does not induce the

formation of solid lead oxide in excess, but rather to a dynamic equilibrium in the intermediate oxygen range [Martynov, 2003]. This observation gives rise to the principle of direct contact steam generator [Martynov, 2003, 2005], as well as to the concept of Pb-Bi cooled direct contact boiling water small fast reactor (PBWR) [Takahashi, 2003]. The accurate knowledge of the possible micro leak rate is critical, as if any, it will most probably exceed all other contamination rates in oxygen. The relation giving the oxidation of lead by water is given in [Martynov, 2005]: oxidation stops once the oxygen activity reaches 10^{-3} of its saturation limits. The potential impact of larger leaks relates to the pressurisation of the cover gas.

The other initial contamination consists in the residual compounds in lead or LBE after manufacturing: it is not the most important one, but represents a source that can be easily dealt with, either by the choice of a "nuclear grade" lead or lead alloy (see Chapter 3), or by the application of specific procedures that would enable to start the nuclear operation with the lowest impurities level achievable.

During the initial start-up, or any restart after maintenance or repair, the oxygen is clearly the largest contamination at this stage of the operation of the nuclear facility [Ivanov, 2003b], [Courouau, 2004c, 2005a]: chemical control and monitoring will enable to control the chemistry of the lead alloys prior to its first irradiation, as well as prior to any operating cycle. Moist air is adsorbed on the residual lead alloys layer as well as on the structural steels in a comparatively high amount that will have to be purified before any restart of the system. This contamination source that was neglected for the first submarine named "project 645", as it was not known, led to the gradual accumulation of oxide in the primary circuit, which eventually concluded, together with the chronic oil leakages of the pumps, to the on-sea accident in 1968 [Ivanov, 2003b]. This accident occurred a few months after the second core have been loaded, and is at the origin of the intensive studies undergone by the Russian related to the liquid lead alloys technology control in the 70s.

The evaluation of the release rates of corrosion products to the liquid metal is rather difficult as it depends firstly on the choice of materials (iron-based steels, ceramics, refractory metals…), on the corrosion mechanisms as well as on the corrosion protection policy chosen (none, self-oxide healing for steels, coating), on the oxygen activity, on the structural materials and on the operating conditions (see Chapter 6). However, the order of magnitude for iron, chromium and nickel for the coolant loop account to a few kilograms per year when iron-based steels would be used for a primary circuit of significant size. This impurities source is then not negligible over years of operations, and should be accounted for, even though it is only roughly assessed for the moment, and variations in the estimations could be very large.

4.3.2 Behaviour of impurities and requirements for purification

As previously listed, most of the contamination by impurities can be expected to remain limited in mass, except for oxygen and corrosion residues. Corrosion products potentially present long-term and cumulative effects, mainly because of the dynamic mass transfer equilibrium that will occur in a non-isothermal system. Pipes clogging due to corrosion products were experienced in several loops which is a specific issue of the HLM: hot or cold stand-by may lead to a rapid redistribution of the deposited impurities within a few hours, eventually clogging the cold pipes as it was observed on the CICLAD loop (see Chapter 12) as illustrated on Figure 4.3.1. This effect was observed within a few hours, as impurities were first accumulated in some cold spot within the loop, then following a change in the loop temperature distribution, the pump duct became the lowest temperature spot in the loop and got plugged. Such observations are reported for almost all research facilities operating with lead alloys and would not be acceptable for any nuclear system.

Figure 4.3.1. CICLAD, Ni pins precipitation in the EMP duct that eventually led to complete plugging

Photo provided by F. Balbaud, CEA Saclay

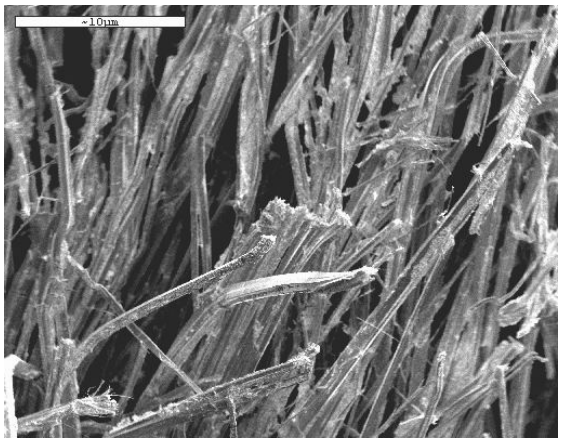

The noble elements, whose oxide are less stable than the lead monoxide, will be dissolved in the liquid metal melt up to their solubility limit, and then be present probably as particles (see Chapter 3). In addition, depending on the level of oxygen controlled in the facility, the impurities might be present either in the oxide or dissolved form according o the Ellingham diagram. In any case, mass transfer from the hot part to the cold part, as well as from the liquid metal bulk to the walls, will occur, thus generating an operating risk for long term operation, so that it is required to propose a continuous purification process to control these continuous contamination sources.

Purification requirements

For a lead-alloy coolant system, which is foreseen to operate for 30 years or longer, as well as for target loop systems, which, due to operating conditions, are expected to be operated only a few years, it appears necessary to trap continuously the impurities in a specific unit. Specific purification campaign during isothermal stand-by and cold shutdown should be foreseen as well.

In principle, only the solid impurities, insoluble particles or oxides should be gathered in a bypass line containing precipitation, filtration,… capabilities. Lower operating temperature will allow minimising the amount of dissolved species. In addition, temperature gradients or packing may promote efficiently crystallisation of these metals and increase the efficiency of the purification unit.

As some homogeneous crystallisation might happens, then, the conditions to provide enough sedimentation and residence time for the existing particles in a cold quasi-stagnant auxiliary vessel should be investigated as an alternative purification system for some specific needs, for example start up purification prior the filling operation. Particles could then be skimmed off from the gas-liquid interface, as most probably some will be settled up at the interface. This interface could be arranged in specific unit, rather than in the loop, as this will affect the gas-liquid equilibrium with non-metallic impurities (O, H…) because of the formation of an oxide film at the interface. It may be a specific issue to assess the localisation of the cold point in a particular system and to compare it to the interface temperature, so as to avoid as far as possible the formation of a thick impurities layer on the interface. This purification by sedimentation is the choice made for the MEGAPIE experiment, prior to its filling operation; where oxides and impurities will be kept in storage vessels [Courouau, 2004c, 2005a], but still require validation.

The filtration system, possibly at the coldest point of the facility, appears as one of the most suitable processes for the lead alloy coolant. This operation is typically a chemical engineering operation, difficult and complex to investigate in liquid metal. Its efficiency depends on numerous parameters, constants or variables during the operations. The main factors of importance are as follows:

- location in the systems, geometry, etc.;
- driving force that induces the flow through the media, regeneration ability;
- operating parameters: flow rate, temperature, etc.;
- solid: nature, form and size, concentration, and particles size distribution;
- filter medium: nature, surface, thickness, pore size, hydrodynamic resistance, mechanical resistance, mode of operation (continuous or batch), pressure and temperature for the filtration, etc.

The particle size distribution defines the choice of the filtration medium. The liquid presenting a large amount of particles of small size (1 μm or less, colloidal) will clog quickly the filtration medium by the formation of little permeable, and compact deposit on the filtration medium ("cake"). The filtration rate will slow down drastically. Particle size distribution might be modified by some process such as coagulation to increase the filtration efficiency. If particles are roughly spherical, the cake will have a good permeability to the liquid, and thus a large filtration rate. Another illustration is available for the elastic or compressible particles, that will act as valves, as any increase of the driving force will decrease the filtration rate, due the compaction of the cake, and a sharp decrease of the pore size [Perry, 1997].

There are typically two types of filtration mechanisms that could be applied to liquid metal technology for separating a solid from a liquid [Perry, 1997]:

- deep bed filtration where solids are trapped within the pores or body of the filter medium;
- cake filtration where solids are stopped at the surface of a filter medium and pile upon one another to form a cake of increasing thickness.

From the lead alloys operating feedback, the following filtering media for deep bed filtration is reported: alumina fibre in the form of textile; glass fibre; metallic mesh textile like or sintered metal filter [Zrodnikov, 2003], [Orlov, 2005].

From the aluminium refinery technologies for advanced applications (aerospace), the use of filtering medium for deep bed filtration, such as alumina foam or zircon-mullite honeycomb medium is reported for the removal of tiny particles before the metal casting operation as once-through operation. In addition, a magnetic field is reported to have promoted the nucleation and crystal growth as well as adsorption on specific metal. There is then a variety of solutions, but, as the basic data are missing, nature of particles, size, form, etc., as well as the filtration rate, so that there neither current design rules or selection criteria are well defined, except for the pressed and sintered fibre metal medium developed for BREST-300 [Papovyants, 1998], [Orlov, 2005].

As the unit will eventually be plugged, it sounds logical either to design the system for the whole service lifetime, or to provide systems with an easy removal and replacement, or regeneration of the filtration medium.

Moreover, nuclear systems purification must be designed to cope with incidental contamination such as the loss of cover gas tightness, water or other ingress (grease, oil, mercury, etc.), as their

impact lays on the loss of operating time because of the need for long and costly purification campaign. In the latter case of contamination, the oil ingress is by far the incident that happened the most often, as in the Prototype Fast Reactor of Dounray (UK-PFR) 1991 (150-200 l). The Russian feedback reports the effect of such an event on lead alloy system (KV-27 land reactor), which is very similar to the sodium-oil pyrolysis reaction giving solid materials [Ivanov, 2003a].

4.3.3 Active impurities

The control of the radioactive impurities topic will not be fully addressed, as it is a complete realm of studies by itself (see Chapter 5), so that only some elements are given hereafter, and particularly supported by one fully documented case study [Petrovich, 2002], in order to sort out which of the active nuclides could be critical for a nuclear system operation, and to focus on some basic hard points for further studies, such as the behaviour of the volatile species (noble gas, Po, Hg, Cs, I), or the mobile species (tritium), or the long half-life nuclides that will affect the maintenance operations during shutdown, and later the waste management for decommissioning. Until now literature insisted mainly on the polonium nuclides production.

4.3.4 Production rates assessment

The activation/spallation sources are continuous and important in term of activities as well as in term of potential dose rate. However, this point should be more fully addressed in order to take provision to the fact that lead is often used as biological shielding to limit the dose rate.

To support the following analysis, figures that were assessed by [Petrovich, 2002] for a primary circuit of a subcritical system, which can be assumed as representative of critical system, as well as for the spallation target circuit, will be taken into account. These calculations correspond to the TECLA project reference subcritical reactor: 300 MWth, 3.7 tonnes of LBE for the target, 2000 tonnes for the LBE coolant loop, 3 mA for the nominal beam current, 0.6 to 1.5 GeV for the beam energy [Courouau, 2003a]. The codes used for the following assessment are MCNPX and SP-FISPACT [Petrovich, 2002].

The most abundant nuclides produced by the spallation reactions are the nuclides close in mass to the lead and bismuth, such as Po, Tl, Hg, and Au, directly descending from the spallation and activation reactions, which basically peel off neutrons from the nucleus. In fact, including all direct reactions and daughter reactions, almost all the periodic table is produced with a clear peak close to the atomic number of the lead or bismuth, and a second one at about half the value. There is about 3 to 4 orders of magnitude difference between the impurities concentrations observed in the target and in the coolant. As regards impurities production, the mass rates are low when compared to other potential source of impurities in the system such as the corrosion source, except for Po in the primary loop where the amount of Bi under the neutron flux is very large, and Po, Hg, Tl, Au, Os and Ir for the target loop:

- target loop: 180 g per operating year (163 g for Po, Hg, Tl, Au, Os and Ir);
- primary loop: 2970 g per operating year (2940 g of Po and 29 g of Tl, Hg, Au and Pt).

As regards the chemistry of these systems, one can only considerer at first the influence of these few impurities:

- target loop: Po, Hg, Tl, Au, Os and Ir;
- primary loop: Po and to a less extent Tl, Hg, Au.

However, possible phenomena occurring in these systems and leading to a local accumulation (plugging), or local effect (corrosion inhibitors or promoters) are to be ascertained, as well as the gas-liquid interactions (Po, Hg, Cs, etc.) and the effect on the control of the dissolved oxygen content.

After one year of irradiation at 3 mA, the total activity of the LBE of the target loop is assessed as being 44300 TBq for the 3.7 tonnes of LBE that makes 12 TBq/kg or 320 Ci/kg. This level of activity appears exceptionally high when considering fluid activity in typical nuclear power plant operation, although it is quite rational in the realm of the high neutrons source. The total activity of the primary loop is assessed as being $1.1\ 10^{18}$ Bq for the 2000 tonnes of LBE, which makes 0.55 TBq/kg or 15 Ci/kg almost only due to ^{210}Bi (52%) and ^{210}Po (43%). The elements giving the highest activities after the coolant and polonium nuclides are the following: Tl, Hg, Au, Pt, Ir, Os, and Re. While the activity of Tl is only about one order of magnitude lower when compared to the coolant, the Re activity is 5 orders of magnitude less. Except for the lead and bismuth isotopes, which represent the coolant activation itself and which are numerous as expected, most of the activity is due to the isotopes of Po, Tl, Hg, Au, Pt, and Ir, listed in decreasing activity order.

Then, after one year of radioactive decay, the total activity of the spallation target decreases by a factor of 35, but is still significant: 1260 TBq that makes 0.340 TBq/kg. Main contributions are the following: ^{210}Po (75% of the total activity), ^{195}Au (9.5%), ^{207}Bi (4.5%), ^{204}Tl (3.5%), ^{195}Os (1.1%) and ^{208}Po (1.5%). The main nuclides responsible for the dose rate are then: ^{185}Os ($3.6\ 10^{6}$ Bq/g), ^{88}Y ($2.55\ 10^{5}$ Bq/g), ^{192}Ir ($2.24\ 10^{5}$ Bq/g), ^{95}Zr ($6.9\ 10^{4}$ Bq/g), with the assumption of a linear relation between the dose rate and the activity.

For the coolant loop, the residual nuclides responsible of 99% of the total dose rate are listed as follows in decreasing order of dose rate contribution: ^{207}Bi(γ β+, 37.97 y – $2\ 10^{4}$ Bq/g supposing a perfect homogeneity within coolant), ^{210}Po (α, 138.4 d – $4\ 10^{7}$ Bq/g), ^{185}Os (γ β+, 93.6 d – 73 Bq/g), ^{208}Bi (γ β +, 3.67 y – 9 Bq/g), ^{144}Pm (γ β+, 363.42 d – 16 Bq/g), and ^{195}Au (γ β+, 186 d – 4500 Bq/g)

To the spallation residues, the activation products should be added for both the coolant and the target loops:

- activation of the coolant, lead and bismuth, which makes up, along with the spallation residues, the largest part of the total activity, as previously illustrated;
- activation of dissolved impurities by the neutron flux, intrinsic impurities from the supplied alloys such as Ag, corrosion products, etc.;
- release of activated products by the corrosion, dissolution of structures submitted to the neutrons.

Then, due to mass transfer and deposition, the activated corrosion products can plate out on different parts of the circuit, being for instance responsible of significant dose rates for the personnel during maintenance and handling operations of some specific component such as pumps, heat exchangers, etc.

To the spallation and activation products, fissions products are released into the primary coolant loop: tritium and fissile products.

Tritium is produced by fission and spallation. This nuclide is rather particular for a reactor system, as it is very mobile throughout hot and metallic interfaces immersed in liquid metal. Although tritium have a low energy activity (beta), it is accounted for as it migrates, is present in section of the reactor where no other radioactive product is expected and is finally released to the environment,

where, as HTO, can have a significant dose impact, if it is not mastered. This is why tritium was studied for the prediction of release rates or inventories in various subsystems, at the time of the design or during operation.

Fissile contamination sources in normal operation are due to surface contamination of the fuel cladding by traces of Pu or U. These traces migrate into the liquid metal, and account for fissile contamination of the coolant. In addition, when subjected to the neutron flux, fission products appear, such as caesium and iodine nuclides, but at very low level. In case of fuel-cladding failure, volatile fission products such as caesium, iodine, xenon and krypton nuclides are released in the system, mostly in the cover gas, in much larger quantities.

4.3.5 Consequences on operations

By contrast to the spallation target which present a small service lifetime with no maintenance nor repairing, the primary circuit is planned for the whole reactor service lifetime (tens of years), which necessarily requires maintenance operations, component handling, refuelling, etc., and might require the use of specific radioactivity control system.

The behaviour of these nuclides depends on their chemical form in the liquid lead alloys:

- dissolved, if the solubility is large when compared to the mass released (Au for instance);
- dissolved, but submitted to precipitation if solubility is low enough in some part of the circuit when compared to the mass released;
- oxidised, if the oxide potential is lower than lead oxide, and depending on oxygen potential of the liquid alloy.

As previously seen, some active nuclides may build-up in specific parts of the system, such as the cold exchange surfaces of heat exchangers, or at the gas-liquid interface, or on other specific spots. This will not have any impact on operations, but during maintenance and component handling, this may lead to the necessity to perform cleaning and decontamination operations.

As the dose rate of the primary coolant is mainly due to ^{207m}Pb, with a level not comparable to any other nuclide, it is critical for designing the biological shielding. However, this nuclide disappears in less than one hour as its half-life is only of 0.8 s, so that other nuclides are to be considered for maintenance or handling operations, and even for the dismantling.

The coolant activation itself influences the operations related to components of fuel handling for maintenance, or repair, as they may require specific operations to allow repair, increasing the overall reactor complexity, as:

- coolant cleaning process to remove the coolant itself;
- decontamination process by acid attack to remove the deposits and first micrometers of the structure, and decrease the activity and dose rate due to nuclides adsorbed into the steel.

In addition, the nuclides, which can transfer from the liquid coolant to another system such as secondary or auxiliary system, cover gas control system, etc., are the main source of concern during normal operating mode, as they may require specific control and processes to keep them within the release authorisations specified by the safety authorities:

- tritium, as it makes up one of the main contribution to the release to the environment;
- volatile species such as Kr, Br, Xe, Ar, I, Cs, H, Po, and Hg nuclides.

Depending on the cover gas system, various solutions can be implemented to control the activities, such as for instance:

- Re-circulating cover gas loop, which can include some delay tanks to increase residence-time and favour radioactive decay of short half-life products (Kr), or trapping on charcoal bed (Xe), or even cryogenic trap, all of which were used for the liquid sodium fast reactor systems. Other specific traps for Po compound or mercury vapour could be designed to reduce coolant activity from those radioisotopes specific to lead alloys system.
- Gas tight system, with venting from time to time to relieve the pressure, with the necessary gas decontamination before release to the stack, as foreseen for the MEGAPIE target operation.

It may be a solution for the polonium nuclides to use their volatility properties (PoPb compound) to eliminate it in the gas phase rather than in the liquid phase, as it could be easier. The effect of the oxygen control process that requires gas flowing to either oxidise or reduce the lead alloys is to be addressed from this activity control issue, as it will affect the gas-liquid distribution of the active nuclides as well. This is especially true for the hydrogen/steam gaseous mixture bubbling or cover gas blowing, as:

- H_2Po, is volatile, so that the process will enhance the Po transfer to the gas phase.
- Tritium, as a hydrogen isotope, will react isotopically with H_2 from the gas phase as well as with the steam, so that the reaction will favour the tritium transfer to the gas phase.

During incidental events, such as the loss of coolant accident, the alpha emitters activity in the lead alloy is often the dimensioning event for the safety scenario. In that case, this allows setting up the specification of the maximum ^{210}Po nuclide that could be agreed in the coolant loop, so as to study and design the necessary control processes [Khorosanov, 2002], [Buongiorno, 2004].

4.4 Instrumentations for chemical monitoring

4.4.1 On-line electrochemical oxygen sensor

The accurate measurement of the oxygen concentration in the liquid lead-bismuth eutectic, as well as in the pure lead alloys for use as coolant in nuclear systems or as liquid spallation target for high neutrons source or accelerator-driven system is a critical issue for defining the active oxygen control that will first of all prevent the contamination of the liquid system by lead and bismuth oxides, as well as, possibly, to ensure an efficient corrosion protection of the iron based alloys structures if the self-healing oxide layer method is chosen.

The use of the ionic conduction properties of some solid electrolyte [Desportes, 1994], and in particular the zirconia based ceramic, allow to make electrochemical cell assembly that allows the measurement of dissolved oxygen in liquid metal system, whose activity could be extremely low ($<10^{-4}$). This is known as the electromotive force measurement in open circuit or as the galvanic cell method.

This technique presents several well-known advantages such as:

- specific to the dissolved oxygen, but the bounded oxygen, such as in oxide, is not taken into account;
- rapid and continuous measurement, that is able to be implemented directly on-line in the system, provided the leak tightness of the seal in between the liquid metal and the ceramic;
- wide concentration range covered by one single sensor, with a lower detection limit that is actually very low, as well as its potential operating temperature range;
- no relation with the size and contact area of the electrodes;
- no disturbance on the measured system.

However, its well-known limitation was its use at a rather high operating temperature, in the order of 750°C typically for a Pt-air reference system, because of the high cell resistance that increases with decreasing temperature, as well as the irreversibility of the cell. In addition, the poor thermal shock resistance requires special care to prevent high thermally induced stresses that can cause cracking of the solid electrolyte. A specific protection from rapid temperature fluctuation shall be provided. Another solution is to design sensor as a consumable item. The service life is often reported as being in the range of the tens to hundreds of hours only.

Although the principle and the application have been well known since the 50s, especially at the laboratory scale for the measurement of basics thermodynamic data, its real application as industrial oxygen sensors began in the late 80s where its applications covered lots of applications, from the automotive industries (lambda sensors) to glove box gas control [Desportes, 1994]. However, some particular and earlier applications such as the sensor for the steel making industry, which is used to measure C/CO ratio, as well as the sensor for the liquid sodium to be used as nuclear coolant (yttria-stabilised thoria), could be noticed [Asher, 1988]. In addition, the Russian institutes developed a specific application for the oxygen control in lead-bismuth eutectic to be used as coolant in nuclear submarines in the late 70s-80s [Gromov, 1997, 1998], [Shmatko, 2000], whose teams paved the ways for this very specific instrumentation in heavy liquid metal coolant with the use of very specific multi layers pellet type sensor [Shmatko, 2000]. This specific design of the solid electrolyte, although very complicated and costly to produce (pellet type, multilayer ceramics, metal to ceramic bonding…), allowed a very accurate measurement of the oxygen together with an exceptionally long service lifetime of 10 years. Some of these sensors are still in use in Russia, as well as in Italy [Azzati, 2003], but are apparently no longer produced. Since the mid-90s, development and testing of new sensor design based on yttria-stabilised zirconia or magnesia-stabilised zirconia were conducted worldwide, including in Russia [Askhadulline, 2003, 2005], [Chernov, 2003], [Colominas, 2004], [Courouau, 2002b, 2004a], [Fernandez, 2002], [Ghetta, 2002], [Konys, 2001, 2004], [Li, 2003], [Muscher, 2001], [Zrodnikov, 2003], [Takahashi, 2002].

The main requirements for an on-line oxygen sensor are as follows: accurate in such a low oxygen concentration range, reliable, predictable and safe for long-term nuclear operation. For instance, one of the main constraints as regards the safety for such system is related to the ceramic breakdown: any leaks of radioactive liquid metal outside the system must be prevented, as well as any ceramic pieces running in the nuclear loop. However, some limitations appeared on some sensors using the commercially available yttria-doped zirconia thimble [Courouau, 2005b], such as the ceramic relative fragility, as well as the time drift that is often observed that will delay for a while their direct implementation on nuclear system. However, the new Russian sensor design [Zrodnikov, 2003] was already used in the nuclear loop of the BOR-60 lead channel [Korotkov, 2003], which operated for

about 100 days. For this sensor, not only the shape (conical when compared to one-end closed tube) but also the composition of the solid electrolyte is adjusted to enhance the ceramic resistance to thermally induced stresses [Askhadulline, 2005].

4.4.1.1 Principle

Sensors are based on the potential measurement method at null current for a galvanic cell built with a solid electrolyte: zirconia doped with either magnesia, calcia or yttria, as this doping element stabilises the ceramic into the tetragonal form that is oxygen ions conducting for a certain temperature and oxygen conditions. Although the Russian feedback indicated the achievement of such sensors for the low operating conditions expected of the lead alloys [Gromov, 1997], [Shmatko, 2000], their assembly was not straightforward at first as it was considered that such electrodes and cells would not work for the temperature of interest for the lead alloys applications (400 to 550°C), because of the irreversibility of the electrode, and because of the too high cell resistance.

The electrodes define either the liquid metal phase where the dissolved oxygen is to be measured, the working electrode, as well as the reference electrode, which is the constant oxygen potential reference system, as illustrated in Figure 4.4.1.

Figure 4.4.1. Galvanic cell principle

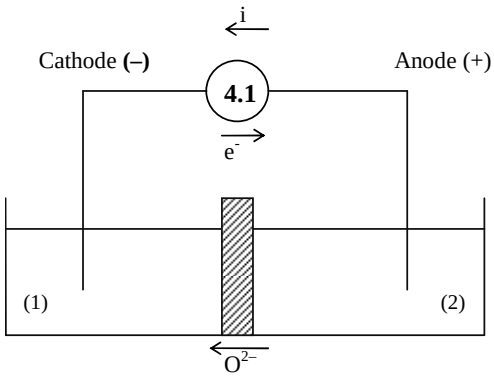

Sensors assembly is made within the laboratory and is now considered as a routine procedure, as illustrated in Figure 4.4.2, where the use of the one-end closed tube allow separating easily the reference (inside) from the measurement medium (outside). One of the critical elements for the design of such sensor is then the sealing between the ceramic tube and the structure of the liquid metal system, which must be leak tight as well as electrically insulated.

Figure 4.4.2. Generic implementation scheme from [Konys, 2001]

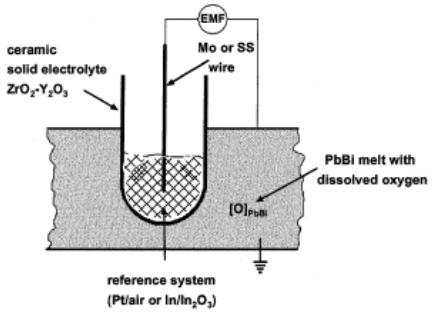

The solid electrolyte supplied by FRIATEC AG company (yttria-doped zirconia, FzY grade, 8.1% in yttria) was used by [Courouau, 2003b] and [Konys, 2001] for instance whereas FERROTROM company supplied the ceramic used by IQS (both magnesia- and yttria-stabilised zirconia) [Colominas, 2004], while some other suppliers can be found worldwide [Li, 2003], or Nikkato Corporation [Ganesan, 2006]. On-purpose ceramic can be synthesised and fired with the required characteristics and shape [Shmatko, 2000], [Askhadulline, 2005]. This supplier list is not exhaustive.

Assembly is done in the open air. Ingots of pure metal and oxides powder are mixed to get a liquid metal internal reference at the operating temperature with only a slight excess of its oxide; 10% to 50% of oxides in excess are reported as satisfactory [Courouau, 2003a]. The air in excess is consumed during the first use, corresponding to the activation of the sensor, to form oxide of the reference metal. The activation of the sensor is done during the calibration procedure or during its first use, the first step of which is the immersion of the sensor in a LBE melt followed by a temperature increase. Once the sensor is giving a stable potential output (electromotive force – emf), the reference is considered at the thermodynamic equilibrium, and the sensor is said activated or ready for operation. This is done in a matter of minutes at 450-500°C.

The choice of the reference system is critical. It depends widely on various parameters [Desportes, 1994], such as the oxygen partial pressure of the reference, which must be close to the partial pressure to be measured, the good knowledge of the equilibrium value of the reference system, a good buffering effect in case of slight disturbances to keep the partial pressure stable, and good compatibility between the lead wire and the reference systems. The use of gas (air, or oxygen) present some advantages, as the partial pressure is accurately known, whereas the thermodynamic data of the liquid metal reference couple metal/metal oxide could be less accurately known, requiring a calibration [Desportes, 1994].

Usually air is used with platinum coated on the ceramic surface for a better junction at the interface, and a Pt lead wire, making the Pt/air electrode, with a well-known limitation in its operating temperature, because of the resistance of the junction between the gas and the solid phase. The operating temperature must be higher than 450°C for such a cell [Desportes, 1994], [Konys, 2004]. To the opposite, liquid metal reference systems provide a better contact with the solid electrolyte, and then a lower cell resistance at comparatively lower temperature. The use of low melting point metal allows favouring the use of the sensor in the required temperature range of a lead alloy system (400-500°C), without an additional heating system.

The effect of thermal cycling on the solid electrolyte when a liquid metal reference is used can be critical. Indeed, the melting /cooling of the internal reference can induce wears on the solid electrolyte, promoting the growth of microcracks, eventually leading to the rupture [Courouau, 2005], whereas the air/Pt electrode used in the same conditions of liquid metal electrode exhibited a much higher service lifetime [Konys, 2004].

The contact lead wire must be compatible with the liquid metal melt of the reference. For instance, molybdenum presents a low solubility in bismuth, which is favourable. To the opposite, platinum or iridium metal, which are the typical lead wired for such electrochemical cell, dissolve in liquid bismuth, forbidding their use on the long term.

The reference electrode must not chemically react with the solid electrolyte, leading to the formation of reaction products on the interface, modifying the potential outputs. Similarly, it must not represent a source of contamination in case of ceramic failure. Bismuth is chemically close to lead, fully miscible, and its oxide is less stable than lead oxide. On the other hand, indium that was used extensively for the Harwell oxygen meter, forms more stable oxide than lead, so that it will reduce the oxygen potential of the liquid lead alloys.

The range of the readings for the indium reference electrode latter system presents a null voltage output, which does not mean that the sensor is broken. This clearly represents an operating difficulty, as in that case, there is no straight possibility to conclude between the effectiveness or the failure of the sensor. An example of that behaviour was observed during STELLA operation (Figure 4.4.5), where the In sensor was believed broken for several days, and several time when its output was close to the null value. This point discards, *a priori*, this reference system for nuclear operation, unless systematic and standard calibration could be developed for a periodic checking of the sensor.

These considerations explain why the choice for the reference systems focused mainly on either the gas system (air-Pt lead wire) or the bismuth (mp. 271°C)/bismuth oxide or indium (mp. 157°C)/indium oxide systems for the reference electrode with Mo as lead wire, although other reference could be used in principle. From the safety point of view, the gas reference system will not be favoured for use in a nuclear system, as it requires the constant flowing of gas inside in the reference electrode, making the route for the contamination of activated lead alloys outside the confinement in case of failure of the solid electrolyte.

4.4.1.2 Theory

This analysis is done for pure lead as well as for the lead-bismuth (55% in weight) eutectic.

The method of the potential measurement with null current can be applied to the measurement of the dissolved oxygen in liquid lead-bismuth alloys. A typical electrochemical galvanic cell that will be subsequently referred to as “EC sensor” is as follows:

Mo, Metal + metal oxide (reference) // ZrO_2 + Y_2O_3 // Pb + PbO (lead alloy solution), steel

where the yttria-stabilised zirconia (YSZ) ceramic, which conducts specifically oxygen ions, separates two medias showing different oxygen activities : an electromotive force (emf) is then formed across the solid electrolyte. If one of the media is defined to act as a reference, so as to maintain constant the oxygen partial pressure to a defined value, then the emf is a function of the oxygen activity in the other medium.

Assuming pure ionic conduction in the solid electrolyte, and assuming that all transfers at the various interfaces developed in the electrochemical cell are reversible, the Nernst relation giving the theoretical emf, noted E_{th}, can be written:

$$E_{th} = \frac{RT}{4F} \cdot \ln \frac{P_{O2(reference)}}{P_{O2}} \tag{4.20}$$

with E_{th} in Volts, R the perfect gas constant (8.31441 J/mol/K), F the Faraday constant (96484.6 C/mol), T the temperature (Kelvin), and P_{O2} the oxygen partial pressure in the lead alloy.

The oxygen partial pressure of the reference, $P_{O2(reference)}$, is defined by the following reaction, in case of a metal (M)/metal oxide (M_xO_y) reference, where x and y are respectively the stoichiometric coefficients for the metal and the oxygen.

$$\frac{2x}{y} M_{(liquid)} + O_2 \Leftrightarrow \frac{2}{y} M_x O_{y(solid)} \tag{4.21}$$

All reactions are written so that it corresponds to the consumption of one mole of oxygen. The units of the free enthalpies of formation are then expressed in J/mol of oxygen O_2.

As the reference is built so as to present a constant oxygen partial pressure, both the metal and its oxide are present in excess to ensure the thermodynamic equilibrium of the reaction. In addition, the liquid solution corresponds to the pure metal, so that the activities of both the reference and its oxide are equal to one and then:

$$\ln P_{O2\ reference} = \frac{\Delta_r G^0_{reference}}{RT} \tag{4.22}$$

The oxygen partial pressure in the lead alloy melt, is given by the thermodynamic equilibrium of lead monoxide, considering that it is the most stable oxide in lead bismuth eutectic.

$$2Pb_{(liquid)} + O_{2(gas)} \Leftrightarrow 2PbO_{(dissolved)} \tag{4.23}$$

The activities product of the lead oxide reaction of formation in lead alloys is then as follows using the oxygen activity defined in Eq. (4.3),

$$\Delta_r G^0_{PbO} = -RT \cdot \ln \frac{a^2_{PbO}}{a^2_{Pb} \cdot P_{O2}} \quad \text{and then} \quad \ln P_{O2} = \frac{\Delta_r G^o{}_{PbO}}{RT} + 2 \cdot \ln \frac{a_O}{a_{Pb}} \tag{4.24}$$

The saturated oxygen concentration for lead and LBE are derived from Eq. (4.1) and Eq. (4.2):

$$\text{Lead: } \ln C^*_{o\,(wgt\%)} = A - \frac{B}{T_{(K)}} \quad \text{with } A = 7.3683 \text{ and } B = 11512.925 \tag{4.25}$$

$$\text{LBE: } \ln C^*_{o\,(wgt\%)} = A' - \frac{B'}{T_{(K)}} \quad \text{with } A' = 2.7631 \text{ and } B' = 7828.789 \tag{4.26}$$

Lead activity is equal to unity in pure lead solution, and is given by the following Russian relation in LBE solution as quoted in [Courouau, 2002b]:

$$\text{LBE: } \ln a_{Pb} = -\alpha - \frac{\beta}{T_{(K)}} \quad \text{with } \alpha = 0.8598 \text{ and } \beta = 135.21 \tag{4.27}$$

The free enthalpies of formation for the various oxides are expressed by the following relations, assuming that all relations are given for the consumption of one mole of O_2:

$$\Delta G^o_{(J/mol)} = \Delta H^o - \Delta S^o \cdot T_{(K)} \tag{4.28}$$

Calculations are made with the help of the HSC database software [HSC, v4.1], which represents a compilation of some of the latest thermodynamic data available. The free energies of formation are linearly regressed on a limited temperature range, 400-1000 K, so as to determine the standards enthalpy and entropy by the least mean squares method. The latter data, standard enthalpy and entropy, are constant over the temperature range (cf. Table 4.4.1)

Table 4.4.1. Main oxides free enthalpies coefficients for the 400-1000 Kelvin temperature range per mole of oxygen O_2 consumed

$\Delta G^{o}_{(J/mol)} = \Delta H^{o} - \Delta S^{o} \cdot T_{(K)}$	**ΔH^{o} (400-1000 K) J/mol**	**ΔS^{o} (400-1000 K) J/mol/K**
4/3 Bi + O_2 = 2/3 Bi_2O_3	-389140	-192.6
2 Pb + O_2 = 2 PbO	-437608	-199.1
4/3 In + O_2 = 2/3 In_2O_3	-618674	-216.8

The general relationship for a metal-metal oxide reference could then be derived from the Nernst relation, assuming a pure ionic conduction in the solid electrolyte:

$$E_{th} = \frac{\Delta G^{o}_{reference} - \Delta G^{o}_{PbO}}{4F} - \frac{RT}{2F} \ln \frac{a_O}{a_{Pb}} \tag{4.29}$$

By using the following constants:

$$a = \frac{\Delta H^{o}_{reference} - \Delta H^{o}_{PbO}}{4F} \tag{4.30}$$

$$b = -\frac{\left(\Delta S^{o}_{reference} - \Delta S^{o}_{PbO}\right)}{4F} \tag{4.31}$$

$$c = -\frac{R}{2F} \tag{4.32}$$

These constants allow to writing down simplified relations:

$$\text{Lead: } E_{th\,(V)} = a + b \cdot T_{(K)} + c \cdot T_{(K)} \cdot \ln a_o \tag{4.33}$$

$$\text{LBE: } E_{th\,(V)} = (a + c\beta) + (b + c\alpha) \cdot T_{(K)} + c \cdot T_{(K)} \cdot \ln a_o \tag{4.34}$$

Hence for saturated oxygen solution, the previous relations depend only on the temperature:

$$\text{Lead: } E^{SAT}{}_{th\,(V)} = a + b \cdot T_{(K)} \tag{4.35}$$

$$\text{LBE: } E^{SAT}{}_{th\,(V)} = (a + c\beta) + (b + c\alpha) \cdot T_{(K)} \tag{4.36}$$

Finally, these general relations could be simplified by using the (a,b,c) constants and the concentration expressed in wt.%:

$$\text{Lead: } E_{th\,(V)} = (a + cB) + (b - cA) \cdot T_{(K)} + c \cdot T_{(K)} \cdot \ln C_{o(wgt\%)} \tag{4.37}$$

$$\text{LBE: } E_{th\,(V)} = (a + c\beta + cB') + (b + c\alpha - cA') \cdot T_{(K)} + c \cdot T_{(K)} \cdot \ln C_{o(wgt\%)} \tag{4.38}$$

The free energies are in good agreement with the respective energies computed with the use of other databases [JANAF], [Barin, 1989]. The slight inaccuracy of these data will affect the theoretical electromotive force calculation by a few millivolts that are assumed as reasonable. Another source of scattering is due to the data coming from the lead activity relation in LBE, which affect only slightly the emf by a maximum of 10 mV, as well as from the oxygen solubility relation, which can affects, on the contrary, the emf to a much greater extent. This is why it is essential to know with a relatively high accuracy the oxygen solubility data (cf. Chapter 3). All calculations presented here are made with Eq. (4.1) and Eq. (4.2) respectively for lead and LBE.

The constants of the Nernst relations can then be calculated, and are reported in the next table for Bi/Bi_2O_3 and In/In_2O_3 reference electrodes for a cell immersed into a lead alloy melt according to the following emf (E) vs. temperature (T) and oxygen concentration (C_o) relationships:

$$E_{(mV)} = K_1 + K_2 \cdot T_{(K)} + K_3 \cdot T_{(K)} \cdot \ln C_{o(ppm\,weight)} \qquad \text{for E > Esat} \qquad (4.39)$$

$$E^{SAT}{}_{(mV)} = K + K' \cdot T_{(K)} \qquad \text{for E = Esat} \qquad (4.40)$$

These relations enables to plot the E vs. T (C_o as parameter) diagram as illustrated in Figure 4.4.3, which are most useful for reading sensor output as well as for calibration of sensor [Konys, 2001], [Gromov, 1998]. It allows plotting the reading easily and to compare the relative position of the oxygen when compared to the PbO saturation line, defining the lower potential value achievable, which must be avoided to keep clear from the contamination by PbO precipitation. Similarly, other oxide stability threshold can be plotted for a direct information on the position of the oxygen potential when compared for instance to the stability of the magnetite.

Figure 4.4.3. Diagram *E* vs. *T* for the oxygen sensor reading in LBE

Indicates the oxygen iso-concentration lines, as well as the PbO saturation and the Fe_3O_4 stability lines for an iron activity of one, the iron oxide being stable below the line. For a lower iron activity, meaning a concentration lower than its solubility, the potential threshold for the dissolution of the magnetite will be lower.

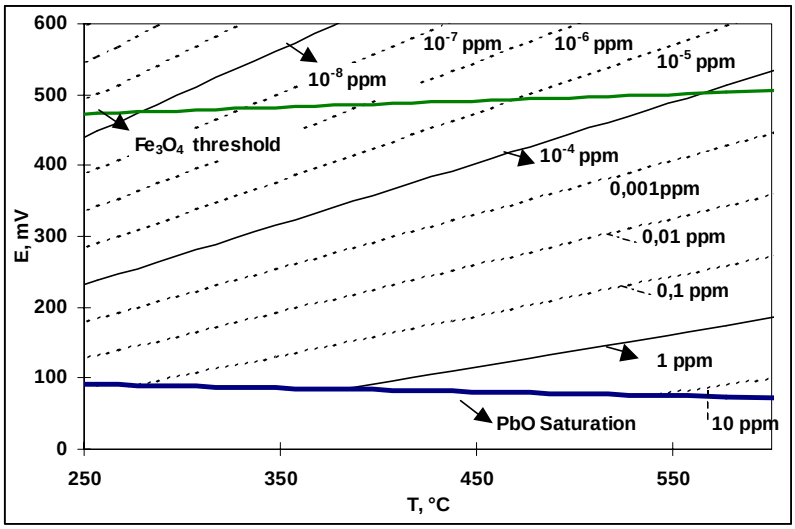

Apart from the data used for the theoretical assessment, there may be other causes for the sensor not to behave according to the theoretical relations: electrolyte conduction properties (slight electronic conduction, impurities in the ceramic, etc.), the influence of the reaction at the electrode/electrolyte

interface (liquid metal/zirconia reaction, or even traces of impurities depositing on the interface), the cell irreversibility (equilibrium not reached due to an oxygen transfer rate limitation especially at very low oxygen partial pressure), as well as the instrumental uncertainties. This is why calibration methods are often required [Subbarao, 1980], [Courouau, 2003b].

Table 4.4.2 synthesises the most useful relations for In and Bi reference sensor in LBE melts.

Table 4.4.2. Theoretical relations for Bi/Bi_2O_3 and In/In_2O_3 references for LBE melts

E in mV, P in bar, T in Kelvin, C in ppm (10^{-6} g/g)

LBE	Bi/Bi_2O_3 reference (melting point 271°C)	In/In_2O_3 reference (melting point 157°C)
$E_{sat}(T)$	$E^{SAT}_{(mV)} = 119.8 - 0.0539 \cdot T$	$E^{SAT}_{(mV)} = -475 + 0.0088 \cdot T$
E (T, a_o), $E > E_{sat}$	$E_{(mV)} = 119.8 - 0.0539 \cdot T - 0.0431 \cdot T \cdot \ln a_o$	$E_{(mV)} = -475 + 0.0088 \cdot T - 0.0431 \cdot T \cdot \ln a_o$
E (T, C_o), $E > E_{sat}$	$E_{(mV)} = -218 + 0.0652 \cdot T - 0.0431 \cdot T \cdot \ln C_{o(wgt\%)}$ $E_{(mV)} = -218 + 0.462 \cdot T - 0.0431 \cdot T \cdot \ln C_{o(ppm)}$	$E_{(mV)} = -812 + 0.1279 \cdot T - 0.0431T \cdot \ln C_{o(wgt\%)}$ $E_{(mV)} = -812 + 0.525 \cdot T - 0.0431T \cdot \ln C_{o(ppm)}$
Ln a_o (T,E) $E > E_{sat}$	$\ln a_o = -23209 \cdot \frac{E_{(mV)}}{T} + \frac{2780}{T} - 1.251$	$\ln a_o = -23.209 \cdot \frac{E_{(mV)}}{T} - \frac{11024}{T} + 0.205$
Ln C_o(T,E) $E > E_{sat}$	$\ln C_{o(wgt\%)} = -23.21 \cdot \frac{E_{(mV)}}{T} - \frac{5049}{T} + 1.512$ $\ln C_{o(ppm)} = -23.21 \cdot \frac{E_{(mV)}}{T} - \frac{5049}{T} + 10.723$	$\ln C_{o(wgt\%)} = -23.21 \cdot \frac{E_{(mV)}}{T} - \frac{18853}{T} + 2.968$ $\ln C_{o(ppm)} = -23.21 \cdot \frac{E_{(mV)}}{T} - \frac{18853}{T} + 12.178$
Ln P_{sat} (T), $E = E_{sat}$	$\ln P^{SAT}_{O2} = -\frac{52362}{T} + 25.67$	
Ln P (T,E) $E = E_{sat}$	$\ln P_{O2} = -\frac{46803}{T} - 46.418\frac{E}{T} + 23.16$	$\ln P_{O2} = -\frac{74413}{T} - 46.418\frac{E}{T} + 26.075$

Using another kind of reference sensor, the air/ platinum reference sensor, described as follows, similar relations could be derived:

Pt, O_2 (reference) // $ZrO_2 + Y_2O_3$ // Pb + PbO (lead alloys solution), steel (4.41)

$$\text{Lead: } E^{SAT}{}_{th\,(V)} = \left(\frac{-\Delta H^o_{PbO}}{4F}\right) + \left(\frac{\Delta S^o_{PbO}}{4F} - \frac{c}{2} \cdot \ln 0.21\right) \cdot T_{(K)} \quad (4.42)$$

$$\text{Lead: } E_{th\,(V)} = \left(\frac{-\Delta H^o_{PbO}}{4F} + cB\right) + \left(\frac{\Delta S^o_{PbO}}{4F} - \frac{c}{2} \cdot \ln 0.21 - cA\right) \cdot T_{(K)} + c \cdot T_{(K)} \cdot \ln C_{o(wgt\%)} \quad (4.43)$$

$$\text{LBE: } E^{SAT}{}_{th\,(V)} = \left(\frac{-\Delta H^{o}_{PbO}}{4F} + c\beta\right) + \left(\frac{\Delta S^{o}_{PbO}}{4F} - \frac{c}{2}\cdot\ln 0.21 + c\alpha\right)\cdot T_{(K)} \quad (4.44)$$

$$\text{LBE: } E_{th\,(V)} = \left(\frac{-\Delta H^{o}_{PbO}}{4F} + cB' + c\beta\right) + \left(\frac{\Delta S^{o}_{PbO}}{4F} - \frac{c}{2}\cdot\ln 0.21 - cA' + c\alpha\right)\cdot T_{(K)} + c\cdot T_{(K)}\cdot\ln C_{o(wgt\%)} \quad (4.45)$$

Finally, these relations are calculated for the saturation using the data previously given using the oxygen concentration expressed in ppm (10^{-6} g/g):

$$\text{Lead: } E^{SAT}{}_{(mV)} = 1133.9 - 0.550\cdot T_{(K)} \quad (4.46)$$

$$\text{Lead: } E_{(mV)} = 637.8 + 0.165\cdot T_{(K)} - 0.043\cdot T_{(K)}\cdot\ln C_{o(ppm)} \quad \text{for E > Esat} \quad (4.47)$$

$$\text{LBE: } E^{SAT}{}_{(mV)} = 1128.1 - 0.587\cdot T_{(K)} \quad (4.48)$$

$$\text{LBE: } E_{(mV)} = 790.7 - 0.071\cdot T_{(K)} - 0.043\cdot T_{(K)}\cdot\ln C_{o(ppm)} \quad \text{for E > Esat} \quad (4.49)$$

4.4.1.3 Calibration

Calibration is based on the comparison of the potential measurements (*E*) with the expected theoretical emf (*Eth*) for defined oxygen concentrations. The main difficulty for lead alloys melt consists in defining exactly the oxygen concentration of the melt. As oxygen is present in traces and subject to the other impurities, so that its actual value is experimentally difficult to assess and to keep stable and particularly on dynamics facilities. Several methods were developed in static conditions based on specific operating procedures to maintain stable the oxygen for a certain delay (temperature variation), or based on chemical equilibrium (dissolved impurity, or gaseous couple),

- the temperature variation close to the oxygen saturation [Konys, 2001], [Courouau, 2002b], as illustrated in Figure 4.4.4, which allow defining accurately the oxygen content of a liquid melt, supposing its concentration stable during the measurement;
- the comparison against metal-metal oxide couple that buffer the oxygen concentration to the equilibrium level [Colominas, 2004];
- the comparison to the known gas phase oxygen content such as the steam/hydrogen gaseous mixture [Konys, 2004] that define the oxygen concentration in the liquid bulk when the gas-liquid equilibrium is achieved.

Another method is based on the coulometric titration method, requiring a well-designed static facility to control all the sources of oxygen contamination. First, the residual oxygen is removed thanks to hydrogen. Then, defined amount of oxygen is added thanks to an electrochemical oxygen pump up to the saturation at a given temperature [Ghetta, 2002].

All of these methods concluded to a rather good agreement between the sensor voltage output and the theoretical emf, and usually justified the use of the theoretical emf relation for the calculation of the oxygen concentration from the sensor readings.

Figure 4.4.4. Oxygen in LBE concentration –temperature diagram illustrating the principle of the calibration by the variation of temperature close to the saturation [Courouau, 2002b], and example of actual calibration points obtained on the ARTOIS gloves box following a specific operating procedure where oxygen remains constant for a while, allowing measuring the inflexion point that defines exactly the saturation temperature allowing to calculate K_1, K_2, K and K′, assuming K_3 constant

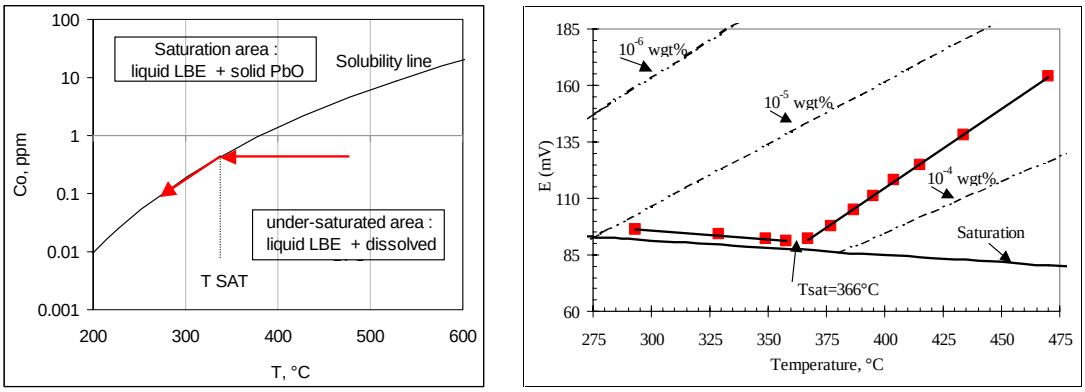

However, a slight scatter of a few millivolts, up to several tens of millivolts is always observed from this theoretical behaviour that is not fully understood yet. The effect of the other impurities might be the source of the errors, by reacting at the solid electrolyte interface and forming metal/metal oxide couple interfering with the electrode potential. This would have to be understood more clearly as this side effect on the calibration process may limit the reliability of the sensors. The second source of errors is interpreted as coming from the zirconia intrinsic properties: slight impurity content variations in the fabrication process may be part of the explanation [Subbarao, 1980].

The temperature variation close to the oxygen saturation calibration method was repeated a large number of times so that mean statistical constants could be derived from it, and are then recommended instead of the use of the theoretical constants [Courouau, 2003b]:

$$Bi / Bi_2O_3 \begin{cases} E^{SAT}{}_{(mV)} = 137 - 0.067 \cdot T_{(K)} \\ E_{(mV)} = -323 + 0.23 \cdot T - 0.0431 \cdot T \cdot \ln C_{o(ppm)} \end{cases} \quad (4.50)$$

$$In / In_2O_3 \begin{cases} E^{SAT}{}_{(mV)} = -412 - 0.051 \cdot T_{(K)} \\ E_{(mV)} = -937 + 0.71 \cdot T - 0.0431 \cdot T \cdot \ln C_{o(ppm)} \end{cases} \quad (4.51)$$

The accuracy is assessed within 5% of the voltage readings (25 mV maximum scattering for a 500 mV reading) that affect the concentration by 40% for the high concentration range to 80% for the low concentration range. Calibration is, in any case, recommended to achieve a better accuracy. However, the availability of a method to achieve a reliable calibration on the field is necessary to significantly increase the accuracy on the long term, as well as to regularly assess the good operation of the sensor.

This is particularly critical as the time drift that was observed on several occasions on static device was recently confirmed by the STELLA loop operation (Figure 4.4.5). The drift appears only after a certain delay of several hundredths of hours, when the lead alloys was submitted to thermal and oxygen variations. Then, the drift gradually and almost constantly increases. In this specific example,

Figure 4.4.5. STELLA absolute time drift observation for two sensors implemented on the same location at the same time (1500 hours of service life)

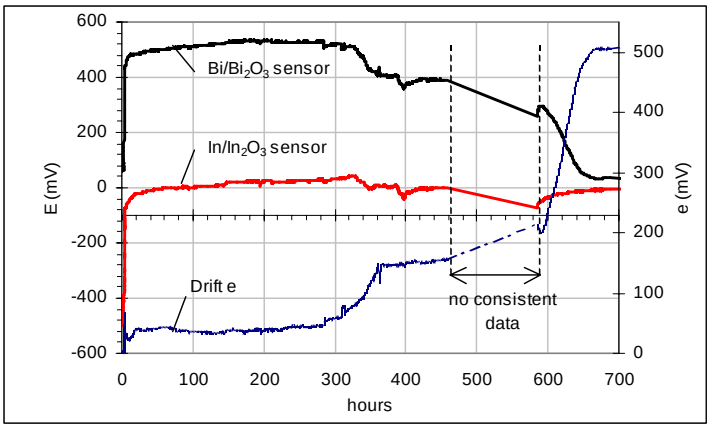

the Bi reference sensor exhibits the highest time drift, while the In reference sensor seems to keep a more consistent reading. The time drift of the Bi sensor is illustrated by plotting on the graph the absolute difference between the theoretical deviation between two different reference electrodes (546 mV here), and the difference between the two sensors readings:

$$e = 546 - \left(E(Bi/Bi_2O_3) - E(In/In_2O_3)\right) \tag{4.52}$$

The value of *e* should be null according to theory, but, in practice, it is always equals to a few tens of mV, except when one of the sensors begins to significantly deviate from its normal behaviour.

Several hypotheses could be proposed to explain this deviation with time [Courouau, 2005b]: alteration of the interface of the electrode (working or reference) by oxide deposition, reaction with the LBE or the liquid metal reference, or alteration on the long term of the solid electrolyte interface by reaction with liquid metals, gases or even oxides. Basic investigation on broken sensor gave no clear results up to now as regards the Molybdenum lead wire, which could thermodynamically be oxidised by the liquid bismuth of the reference electrode, as the relative stability of the potential oxide is as follows: $In_2O_3 > MoO_2$, $MoO_3 > Bi_2O_3$ [Li, 2004].

The time drift understanding as well as the development of on-the-fields calibration method will enhance the overall sensor reliability, which are the basis of the ongoing research.

4.4.1.4 Characteristics of the oxygen sensors

Sensors have been tested for thousands of hours in both static and dynamic conditions in stable and unstable chemical conditions that validate their effective and reliable use for dynamic loop operation [Askhadulline, 2005], [Ghetta, 2002], [Colominas, 2004], [Courouau, 2003b], [Gromov, 1997], [Konys, 2004], [Shmatko, 2000]. These tests allowed gaining a large operating feedback representative of long-term operations on a wide variety of operating conditions. The characteristics observed up to now on these oxygen prototypes sensors are then satisfactorily and confirm the previous observations, as regards the operating range (370°C-550°C for the Bi/Bi_2O_3 reference electrode), the oxygen concentration range, the response time, the accuracy and reproducibility, as well as the service life (several thousands of hours, longer expected in stable conditions). A lower operating temperature than 350°C is possible but with a lower accuracy as the sensor outputs deviate from ideal behaviour most probably because of an increasing irreversibility of the cell.

The time to react to a concentration change is fast for an oxygen contamination. The recovery time is linked to the chemical reaction kinetics that is limited by the mass transfer phenomenon (gas-liquid interface, oxygen diffusion in liquid bulk…). From a general point of view, the transient phase of one system is not absolutely reliable as the oxygen content is globally inhomogeneous. However, this effect disappears in steady state conditions. The sensor gives only the local oxygen content, so that the loop implementation is important to get reliable information of a homogenous system [Orlov, 2005].

The time drift is negligible with low oxygen concentration ($<10^{-6}$ ppm) and stable operating conditions. Higher oxygen content ($>10^{-6}$ ppm), or oxygen cycling, seems to affect the sensor output, reducing its service life. The other impurities present in the liquid metal may play a role as well. Another explanation is related to the electrolyte limitation itself. This could be solved by a cleaning operation (high temperature in low oxygen content, or, to be tested, a nitric acid washing of the zirconia). This is a point to be further studied, as this would possibly require a calibration procedure suited for loop operation, an on-the-field procedure, that is not available yet, as well as, if possible, a specific and complex regeneration procedure.

Although yttria-doped zirconia is known to present a better thermal shock resistance (temperature gradient, temperature cycling) as well as a better mechanical resistance when hot (vibrations, contact, etc.) when compared to other solid electrolytes such as yttria-stabilised thoria, a number of failures has been observed (Figure 4.4.6). The point of breakdown is often observed at the central point localised at the bottom of the ceramic thimble. The internal reference electrode when localised in a closed-end tube is itself a source of major mechanical wear during its solidification. Optic observations of the ruptured ceramic surface (Figure 4.4.6) indicate the gradual insertion of bismuth into microcracks most probably due to the positive volumetric change of Bi during its solidification. Lowering the height of the internal reference electrode will reduce this effect. The use of conical shape for the solid electrolyte is most favourable from this particular point of view, as the solidification constraints will exert preferentially upwards towards the free level rather than radially towards the ceramic. This conclusion is further evidenced by the experimental observations from the CORRIDA loop [Konys, 2004]: the air/Pt reference sensor exhibited a much higher service lifetime when compared to the Bi/Bi_2O_3 reference sensor used within the same operating conditions, and with the same electrolyte.

Figure 4.4.6. Bi/Bi_2O_3 sensor operated for 1400 hours on the STELLA loop and details of the point of rupture [Courouau, 2005b]

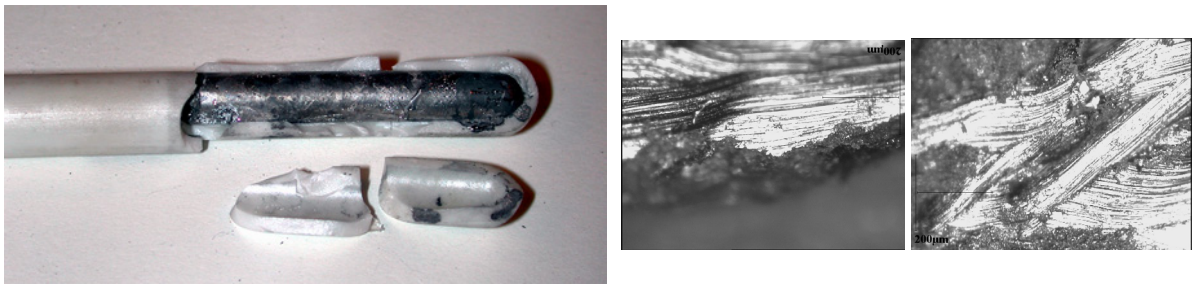

Another method to increase to reduce failures is to use a proper design for the ceramic housing, together with the use of special procedure for operation. This was typically used for the liquid sodium sensor (Westinghouse, Harwell) and is known as efficient [Asher, 1998]. Figure 4.4.7 presents one of the design for such a housing that has been achieved [Courouau, 2005b], and that must be validated on the STELLA loop. A similar design is used at the Karslruhe Lead Laboratory [Konys, 2001]. Its main characteristics consist in having the seal ensuring the tightness of the facility between the ceramic and the metallic structure localised in the cold area, which is made possible thanks to the ceramic length,

Figure 4.4.7. CEA sensor housing to be tested on the STELLA loop [Courouau, 2005b]

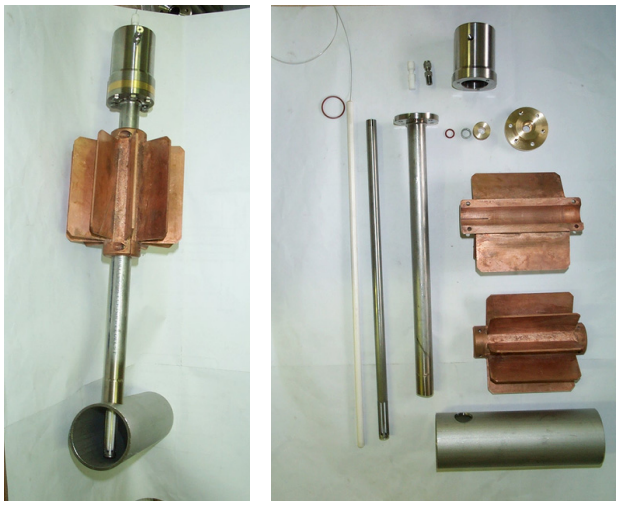

and thanks to the copper fins. The seal is then a simple O-ring. The ceramic is protected with a metallic sheath reducing shocks, both thermal and mechanical, and keeping ceramic pieces in case of rupture. Leak detection is ensured at the cap location with a specific temperature measurement. Any liquid metal coming up there should in principle stay confined thanks to this metallic cap.

This kind of design proved efficient in liquid sodium technology, as the sensor service lifetime was not depending from the sealing medium, which, if localised in the bottom area, would be in contact with high temperature liquid metal, eventually leading to a short circuit, or the loss of the leak proofness.

Although the closed-end tube shape is commercially available and easily separates the two electrodes, the working and the reference electrodes, it might have to be replaced by other less fragile shapes, like a conical shape sealed with graphite or tantalum [Li, 2003] or fused with a metal to ceramic bound [Chernov, 2003] to a metallic tube that is reported as far more resistant. However, the implementation becomes more complex because of the issue of the metal-to-ceramic sealing and fusing, without speaking of the cost of the specific fabrication of ceramic pieces. The Russian model, dating from the early 90s, and which is now registered in the Russian state standard committee (Figure 4.4.8), was, for instance, implemented on the BOR-60 lead channel and operated most satisfactorily during the irradiation time [Korotkov, 2003]. Recent developments include the inclusion of impurities, such as particles of alumina (nano size), as well as the specific firing procedure to exceptionally improve the mechanical resistance of the solid electrolyte [Askhadulline, 2005]. The more recent US model (Figure 4.4.9) is based on the solid electrolyte used in the car industry for the lambda sensor, whose ceramic part is then quite widely available at low cost. It is awaiting long-term validation in representative conditions for the long-term behaviour of the seal. In additions, a reactive braze for the bound was recently developed within the framework of a specific MIT-Ceramtec agreement with promising results up to now [Ballinger, 2006].

4.4.1.5 Conclusions

The oxygen monitoring system is quite compulsory for any lead alloy systems at least to ensure the contamination control. It is now clear that sensors based on solid electrolyte electrochemical cell proved efficient for measuring the dissolved oxygen of the lead alloys systems, despite a number of

Figure 4.4.8. A schematic cross-sectional view of the oxygen sensor developed by IPPE [Zrodnikov, 2003]

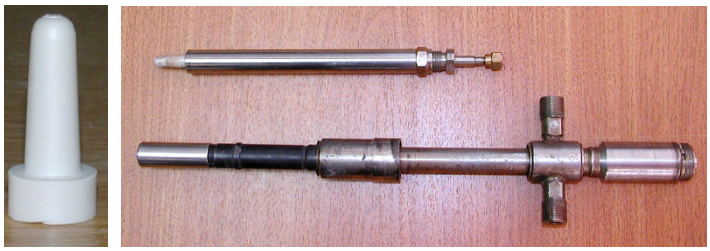

Figure 4.4.9. LANL ceramic element with the graph-lock gasket and the metallic sheath with the seating ring [Li, 2003] and the reactive braze bound [Ballinger, 2006]

limitations, which are quite typical of this kind of measurement. However, it is not commercially available, so that for a day-to-day use on experimental facilities, the theoretical background and know-how given in this section will allow the assembly of sensor from available part, as well as its basic use and allow interpreting its outputs.

Several concepts were designed and are presently at different level of achievement, but all are under rapid progress for a reliable use in a nuclear system. One can notice in particular the outstanding level of achievement of the Russian design, which presents, apparently, none of the limitations identified and described in this section, and was successfully used in a nuclear environment.

4.4.2 Development of sampling systems and analytical methods

The impurities monitoring system for the liquid phase is typical of the liquid metal fast reactors: a system that allows getting a liquid metal sample, in order to perform a chemical or radiochemical analysis of the impurities. A periodic sampling enables in principle to monitor the behaviour of the dissolved impurities on the long term as well as to assess the gradual activation of the coolant.

4.4.2.1 Dip sampler validation

There are two main different types of sampling system:

- dip sampling throughout an airlock system, which is the reference sampling system in liquid metal reactors such as the sodium-cooled;
- circulation in a tube-sampling device in a bypass line, which was partly given up because of representativeness difficulties as regards the corrosion products (potential accumulation due to deposits on the walls), although this is questionable depending of the impurities to be measured.

The objective is to be able to take a sample of liquid LBE in any facility to perform subsequent chemical analysis of the impurities. The following specifications are usually required for any sampling system:

- to obtain an homogeneous liquid metal sample;
- to provide a sampling system that do not pollute liquid metal sample;
- to design an easy-to-use system that complies with a nuclear environment;
- to provide a system that may be quickly cooled.

Such a device was already developed for the lead-lithium eutectic alloy that is studied for the tritium-breeding blanket of fusion reactor [Desreumaux, 1993]. The basic principle was to adapt the sampler to the LBE melt and achieve a first qualification on a static facility. The scheme and a view of this dip sampler developed for the lead-lithium alloy is provided hereafter (Figure 4.4.10) together with the LBE sample obtained [Courouau, 2002a].

Figure 4.4.10. Scheme, view of the dip sampling system, which is then hooked to a stem and immersed throughout an air lock, as well as the resulting LBE sample

The tube on the bottom part, opposite to the hole for the inlet of the melt, was necessary to ensure a good filling of the sampler by enabling degassing. This tube is not really needed for lead-bismuth alloy because of its higher density. The dip sampler fabrication could then be simplified. The stripy marks done during fabrication on the external surface of the dip sampler enable, in principle, an easy discarding of the steel, like the opening of a tin, delivering the LBE sample ready for its analysis.

The nature of the material used up to now is stainless steel. Its effect on the dissolved impurities content was not assessed. However, a material pure and presenting very low solubilities in lead alloys is recommended. Elements such as Fe, Cr, Nb, Mo, Co, Ti, Si and Zr present very low solubilities in the liquid lead-alloys eutectic, and could be efficiently used for the dip sampling material. However, as Fe and Cr are two of the impurities to be analysed, it is recommended to avoid them for the candidate material. Carbon in the form of graphite or composite like SiC can possibly be used.

The issue of the representativeness of the measurement has not been treated due to the lack of any sampling in loop operating conditions. This issue is to be further investigated, as the sampling system might not be homogeneous for all nuclides. Indeed, some impurities might be concentrated on the walls

of the sampling system, so that the conditions of sampling (temperature, immersion time, temperature decrease gradient, etc.) are to be optimised on the basis of the future experimental feedback. In addition, the topic of the possible contamination of the sampling system during the immersion by the free surface oxides is not addressed. The feedback from past development should be taken into account for the liquid metal sample optimisation, such as for instance multiple sampling systems for a larger amount of metal sampled such as the "harp sampler" (Figure 4.4.11) [Borgstedt, 1989], and especially for a technique and know-how developed for achieving representative sampling [Borgstedt, 1989]. The use of alternative techniques, such as on-line distillation technique that was once studied and applied for the liquid sodium, should be reassessed.

Figure 4.4.11. Schematic drawing of an overflow multiple sampler for flowing alkali metals, the "harp sampler" [Borgstedt, 1989]

1 – fittings, 2 – sampler, 3 – sampler drain pot, 4 – crucible

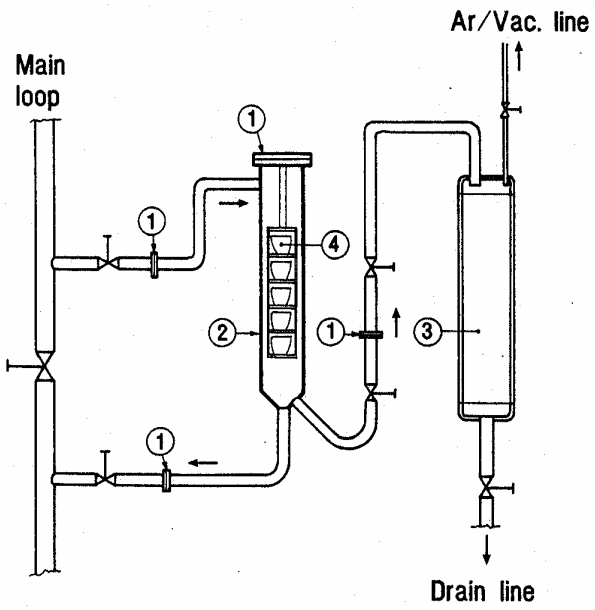

4.4.2.2 Chemical analysis of lead-bismuth eutectic

Various techniques are used for lead alloy characterisation, as follows [Desreumaux, 1998]:

- composition analysis;
- characterisation of metallic impurities;
- oxygen present in the alloy measurement;

The composition analysis techniques are based on calorimetry, surface spectroscopy analysis, or atomic absorption spectroscopy (AAS). The calorimetric method principle is to measure the thermal flux absorbed or produced by a sample subjected to a temperature increase. The results enable deducing the respective reaction temperature, the eutectic and peritectic points, as well as the reaction specific heat. But this kind of analysis is not sufficient by itself as several compositions are often possible when referring to a phase diagram.

The surface spectroscopy analysis consists of X-ray analysis, scanning electron microscopy (SEM), or wavelength dispersive X-ray fluorescence (WDXRF). When energy dispersive X-ray spectrometer (EDS) is coupled to a scanning electron microscope, the measure of the alloys composition is possible in any point of the surface of the sample. Mean value of several points (10 at least) could be used to determine the mean composition of the alloys. The scanning electron microscope enables determining the general state of the alloys, through the study of its enriched or depleted zone. The latter method, WDXRF, enables the measurement of virtually all the periodic table (Z > 11) for concentrations above 500 μg/g [Desreumaux, 1998]. This method is thus well adapted to the alloy composition determination, but not for the measurement of impurities.

The metallic impurities analyses are achieved first by dissolution of the lead alloy, and then by the use of inductive coupled plasma/mass spectrometry (ICP/MS) or AAS. The ICP/MS method enables the measurement of a wide range of impurities such as Fe, Ni, Cr, Ag, Cd, Cu, Sn, Sb,…

The iron impurity has an isobaric interference with ArO gaseous mixture (Ar being the plasma gas) that increases the lower detection limit to 50 μg/g. For the iron impurity, the AAS technique coupled with the spiking method is then a better choice than the ICP-MS technique, resulting in a lower detection limit decreased to 5 μg/g.

For the nickel impurity, because of the contamination coming from the nickel cones of the transfer chamber of the ICP/MS apparatus, the lower detection limit is high when compared to the other impurities. There are two methods for decreasing the lower detection limit: changing the cones to platinum cones, or measuring nickel by AAS with spiking method that decreases the lower detection limit to 5 μg/g as well.

The analytical measurement of oxygen in a sample can be made by two methods [Desreumaux, 1998]. The first method is based on the reductive fusion of the sample in a graphite crucible. The resulting carbon dioxide is measured by infrared spectroscopy. This technique is used with careful calibration in the expected range, and with devoted preparation procedures for the sample in order to reduce any superficial oxide. It measures the total amount of oxygen present in the alloys: either the dissolved oxygen or the oxides. The other method is based on electrochemical measurement as described in the next subtask with laboratory scale electrochemical cells. It measures only the dissolved oxygen present in the liquid metal solution.

The methods were applied to LBE samples performed on the alloy supplied by METALEUROP to CEA Cadarache [Desreumaux, 1998] (Table 4.4.3).

Table 4.4.3. Composition of the METALEUROP LBE

	Calorimetry		**WDXRF**	
	Melting point	**Enthalpy**	**%Pb**	**%Bi**
Measurements	126.2°C	17.0 J/g	41.7±2	57.3±2

Table 4.4.4 gives the impurities measured, as well as the values of the pure lead and bismuth characterised by the supplier for comparison. During the cooling phase of the dip sampling, a segregation phenomenon occurs, resulting in a relative heterogeneity of the lead alloy depending on the method used for composition characterisation. Typically, a better composition measurement is obtained by dissolution of the whole sample, than on parts of the sample.

Table 4.4.4. Metallic impurities measured in the METALEUROP LBE

	Analytical technique	EPB measured (μg/g)	Bi (theoretical) (μg/g)	Pb (theoretical) (μg/g)
Sn	ICP/MS	<2	<1	<2
Fe	AAS	<5	<1	
Ni	AAS	<5	1.4	<1
Ag	ICP/MS	3	1	6
Cu	ICP/MS	<2	<1	<2
Zn	ICP/MS	<2	<1	
Cd	ICP/MS	<1	<1	<2
Sb	ICP/MS	<2	<3	<2
As	ICP/MS	<2	<1	<2
Te	ICP/MS	<1	<1	<3

The table provides the metallic impurities concentrations measured in the alloys with the different analysis techniques. This compares well to one of the other characterisation available [Glasbrenner, 2004b] made on the LBE supplied by Impag AG (Switzerland) which contained a few ppm of impurities: Ag 11.4, Fe 0.78, Ni 0.42, Sn 13.3,Cd 2.89, Al 0.3, Cu 9.8, Zn 0.2.

The first tests for the oxygen measurement were made with a LECO apparatus calibrated with steel matrix giving thus a different fusion temperature. The results showed dispersed values for the lead alloy sample: from 1 μg/g to 5 μg/g. A different approach based on calibration of the apparatus with a 1 μg/g lead sample did not allow lowering the detection limit. Actually, the apparatus used for these measurements proved insufficient for this kind of study: background level of the LECO apparatus is too high and its resulting sensitivity appeared too low when compared to the effective operating oxygen concentration range (0.01 ppm).

4.4.2.3 Radioactive nuclides chemical analysis

The regular radio activation measurement of the coolant is typical for nuclear system operation, as it can affect the reactor operation (handling or repair during maintenance operation, fuel-cladding failure, transfer or accumulation on specific part of the system…). All nuclides being gamma emitters can be measured by gamma spectrometry. This is typically achieved after having dissolved the metal sample in an aqueous solution (nitric acid). However, other nuclides, which are specific to the spallation reaction, or due to the activation of the heavy liquid metal coolant, are only beta-emitters (most of the Bi, Tl, Hg, Au, Pt nuclides), or even alpha-emitters (^{208,209,210}Po). Their measurement requires then specific procedure in order to be able to measure traces, and in some case to be able to measure each of the isotopes produced for one particular nuclide (Po).

Preliminaries investigations were achieved for the Po isotopes speciation by [Lacressonniere, 2003] that was applied to one of the first LiSoR irradiated sample (36 hours, 2002). Measurements gave: 3752 Bq/g of ^{208}Po, 22 Bq/g of ^{209}Po, 19 Bq/g of ^{210}Po, which corresponds to the measurement achieved independently by the Paul Scherrer Institute [Glasbrenner, 2004b], as well as to the nuclear production assessment. The technique is based on concentration of the nuclides in a first step (ferric co-precipitation, and liquid-liquid extraction with tri-butyl-phosphate), then in a second step by the self-deposition on an argent disk for alpha-spectrometry measurement.

The technique that was under study for the traces measurement of the mercury concentration is the atomic absorption spectrometry coupled with a vapour generator. The detection limit achieved by this method is 0.06 ppm (60 10^{-9} g/g) [Chabert, 2003].

4.4.2.4 Conclusions

The dip sampling system that was originally developed for Pb-Li alloys got a first validation in LBE. The issue of the representation is to be further assessed, in order to eventually propose an optimised design. Indeed, the sample must be representative of the liquid metal bulk, which is depending of the location of the sampling, and then of the design of the nuclear system.

The analytical techniques for metallic impurities measurement: Fe, Ni, Cu, Sn, Ag, Zn, Cd, Sb, As, Te, for which either ICP-MS or AAS with spiking method have been used, were as well demonstrated. However, the lower detection limit of 5 ppm cannot be further lowered, unless another ICP-MS apparatus, more costly, is used to lower the detection limit by one order of magnitude: 0.5 ppm. Industrial analytical laboratories are usually equipped with such equipment. A cross-comparison benchmark with such laboratories is necessary, however, to confirm the lower detection limit and accuracy of the measurement, including, in particular all the crucial preparation steps of the samples.

Concerning the radioactive impurities, measurement techniques were developed only for the speciation of the polonium and mercury, as the techniques for low alpha or beta activities measurement are not straightforward. Further developments for the speciation methods should concern the main spallation and activation products isotopes that are expected for normal operating conditions: Po, Bi, Pb, Hg, Au, Pt, Ir, Re, Ta, Hf. The techniques for solvatation, concentration, etc., are part of the development envisaged.

However, during normal operating conditions in an anisothermal system, the equilibrium concentration of the main impurities involved in the corrosion and mass transfer processes will be lower or even far lower than the lower detection limit available (5 ppm or even 0.5 ppm). This makes really difficult the iron monitoring, for instance. There is no straight solution foreseeable to solve that issue, except the use of an indirect measurement method. Indeed, the steel making industry uses the oxygen measurement to check the dissolved carbon, as the dissolved oxygen is defined by the C/CO chemical equilibrium in that particular condition. Detecting the iron oxide stability threshold, providing the availability of precise data and good sensor accuracy could be one of the solutions.

4.5 Conclusions

The chemistry control in a nuclear system appears as a quite complex issue, and particularly critical to keep under control the corrosion in a wider operating temperature range, as well as to keep the coolant free of any contamination by oxides, which is basically the first requirement. The radiochemistry control appears as well as difficult, as, production rates are relatively inaccurate, and as the transport phenomena as well as associated purification processes are to be more understood and developed.

However, the chemistry control is usually not critical for operation if it was taken into account at the early stage of the design as well as during the start-up and shutdown procedures. This is why it should not be neglected in designing any kind of systems, especially in the view of the potential operating difficulties that could result from it. Well-designed and well-operated facilities could be run, in principle, with a rather high confidence, in the no-oxygen conditions. Higher operating temperatures require the validation of oxygen control systems at a specified medium range concentration on the long term for larger systems, and especially for pure lead.

There are some similarities in the chemistry analysis of water, liquid sodium and lead alloy systems. They all present quite identical requirements for both monitoring and processes. However, the consequences for an LBE system are much more critical, such as the loss of cooling capacity due to plugging or the loss of confinement due to corrosion, which makes this issue as one of the most important one when operating such system.

Some points remains open for further studies, such as the process optimisation of oxygen control systems, the improvement of the reliability of the associated instrumentation, such as the oxygen sensor, as well as the basic phenomena for aerosols, particles and mass transfer, even of impurities present in traces such as the active contaminants, within a close and tight system on the long term, for which the basic understanding should be increased.

REFERENCES

AEN-NEA report n°5419 (2005), *Fuels and Materials for Transmutation – A Status Report*.

Asher, R.C., D.C. Harper, T.B.A. Kirstein, F. Leach, R.G. Taylor (1988), "Recent Developments in the Design, Performance and Application of HARWELL Oxygen Sensors and Harwell Carbon Meters", *4th International Conference on Liquid Metal Engineering and Technology (LIMET)*, Avignon, France, 17-21 Oct.

Askhadullin, R.S., P.N. Martynov, *et al.* (2005), *Development of Oxygen Sensors, Systems of Control of Oxygen Content in Lead Coolants for Test Loops and Facilities*, International Science and Technology Centre, contract n° 3020.

Askhadullin, R.S., P.N. Martynov, A.A. Simakov, Z.I. Emepiantseva, O.M. Sisoev, V.S. Lanskikh, V.A. Gulevskiy, M.E. Chernov (2003), "Regulation of the Thermodynamic Activity of Oxygen in Lead and Lead-bismuth by the Dissolution of the Oxides in Heat Transfer Systems", *Proceedings of the Fast Neutrons Reactors Conference*, Obninsk, Russian Federation, Dec. 8-12 (in Russian).

Azzati, M., A. Gessi, G. Benamati (2003), *Experimental Results on Oxygen Control Systems – TECLA D28*, ENEA FIS ENG Technical Note, December 5th.

Balbaud-Célérier, F., F. Barbier (2001), "Investigation of Models to Predict the Corrosion of Steels in Flowing Liquid Lead Alloys", *Journal of Nuclear Materials*, Vol. 289, pp. 227-242.

Ballinger, R.G. (2006), private communication.

Ballinger, R.G., J. Lim (2004), "An Overview of Corrosion Issues for the Design and Operation of High Temperature Lead and Lead-bismuth Cooled Reactor Systems", *Nuclear Technology*, Vol. 147, pp. 418-435.

Barin, I. (1989), *Thermochemical Data of Pure Substances*, VCH Editions, Weinheim Germany.

Blochin, V.A., E.G. Budylov, R.I. Velikanovitch, I.N. Gorelov, A.N. Deryugin, Z.I. Ievleva, M.I. Kosina, Y.A. Musihin, I.D. Ponimash, A.D. Sorokin, A.L. Shimkevich, B.A. Shmatko, E.G. Shcherbakov (1998), "Experience of Development and Operation of Oxides Electrolytic Sensors in Lead-bismuth Coolant", *Proceedings of the Conference of the Heavy Liquid Metal Coolants in Nuclear Technology*, Obninsk, Russian Federation, 5-9 October, pp. 87-100 (in Russian).

Borgstedt, H.U., C.K. Mathews (1987), *Applied Chemistry of the Liquid Alkali Metals*, Plenum Press, New-York-London.

Borgstedt, H.U., Z. Peric (1989), "Sampling of Alkali Metals in Nuclear Applications", *Erzmetall*, Vol. 42, No. 11, pp. 504-507.

Buongiorno, J., E.P. Loewen, K. Czerwinski, C. Larson (2004), "Studies of the Polonium Removal from Molten Lead-bismuth for Lead Alloys Cooled Reactor Applications", *Nuclear Technology*, Vol. 147, pp. 406-417.

Buongiorno, J., N.E. Todreas, M.S. Kasimi (2002), "Heavy Metal Transport in Lead-bismuth Cooled Fast Reactor with In-vessel Direct Contact Steam Generation", *Nuclear Technology*, Vol. 138, pp. 30-43.

Chabert, C. (2003), personal notes.

Chernov, M.E., P.N. Martynov, V.A. Gulevskiy (2003), "Development of Electrochemical Capsule Oxygen Sensor for Control and Monitoring of Heavy Metal Coolant Condition", *Proceedings of the Fast Neutrons Reactors Conference*, Obninsk, Russian Federation, 8-12 Dec., (in Russian).

Colominas, S., J. Abella, L. Victori (2004), "Characterisation of an Oxygen Sensor Based on In/In2O3 Reference Electrode", *Journal of Nuclear Materials*, Vol. 335, pp. 260-263.

Courouau, J-L. (2000), "Oxygen Control Systems, Comparison Between Oxygen Probes", *Proceedings of the 1st MEGAPIE Technical Review Meeting*, Cadarache, France, 14-15 June.

Courouau, J-L., P. Trabuc, *et al*. (2002a), "Impurities and Oxygen Control in Lead Alloys", *Journal of Nuclear Materials*, Vol. 301, pp. 53-59.

Courouau, J-L., P. Deloffre, R. Adriano (2002b), "Oxygen Control in Lead-bismuth Eutectic: First Validation of Electrochemical Oxygen Sensor in Static Conditions", *Journal de Physique IV*, France 12, Pr8, pp. 141-153.

Courouau, J-L. (2003a), *Impurities and Purification Processes in Lead-bismuth Systems*, Deliverable No. 25, TECLA, 5th EURATOM Framework Programme No. FIKW-CT-2000-00092.

Courouau, J-L., L. Pignoly, C. Delisle, P. Deloffre, F. Balbaud (2003b), *Report on the Long Term Validation of Electrochemical Sensor*, Deliverable No. 32, TECLA 5th EURATOM Framework Programme No. FIKW-CT-2000-00092.

Courouau, J-L. (2004a), "Electrochemical Oxygen Sensors for On-line Monitoring in Lead-bismuth Alloys: Status of Development", *Journal of Nuclear Materials*, Vol. 335, pp. 254-259.

Courouau, J-L., J-C. Robin (2004b), "Chemistry Control Analysis of Lead Alloys Systems to be Used as Nuclear Coolant or Spallation Target", *Journal of Nuclear Materials*, Vol. 335, pp. 264-269.

Courouau, J-L., S. Sellier, F. Balbaud, K. Woloshun, A. Gessi, P. Schuurmans, M. Ollivier, C. Chabert (2004c), "Initial Start-up Operations Chemistry Analysis for MEGAPIE", *Proceedings of the 5th MEGAPIE Technical Review Meeting*, Nantes, France, 24-26 May.

Courouau, J-L., P. Agostini, P. Turroni, H. Glasbrenner (2005a), "Review of the Oxygen Control for the Initial Operations and Integral Tests of the MEGAPIE Spallation Target", *Proceedings of the 6th MEGAPIE Technical Review Meeting*, Mol, Belgium, 27-29 June.

Courouau, J-L., S. Sellier, C. Chabert, L. Pignoly (2005b), "Electrochemical Oxygen Sensor for On-line Measurement in Liquid Lead Alloys Systems at Relatively Low Temperature", forthcoming in *AFINIDAD, Journal of Theoretical and Applied Chemistry*, Chemistry Institute of Sarria (IQS), Barcelona, Spain.

Desportes, C., M. Duclot, P. Fabry, J. Fouletier, A. Hammou, M. Kleitz, E. Siebert, J-L. Souquet (1994), *Électrochimie des solides*, EDP sciences – Presse universitaire de Grenoble, ISBN 2.7061.0585.1 (in French).

Desreumaux, J. (1998), *Caractérisation de lingots d'alliage Plomb-Bismuth de deux provenances différentes*, Technical Note CEA DER/STML/LEPE 98/061 (in French).

Desreumaux, J., C. Latgé, J. Le Texier, S. Poinsot (1993), "Development of a New Plugging Indicator and Experimental Tests in a Lithium-lead Facility", *Conference on Liquid Metal Systems*, Karlsruhe, Germany, 16-18 March.

Fazio, C., M. Azzati, G. Benamati (2000), *Oxygen Control Strategies in Large Loop, Critical Analysis of the Different Process*, ENEA FIS ENG Technical Note HS-A-R—007.

Fernandez, J.A., J. Abella, J. Barcelo, L. Victori (2002), "Development of an Oxygen Sensor for Molten 44.5% Lead_55.5% Bismuth Alloy", *Journal of Nuclear Materials*, Vol. 301, pp. 47-52.

Ganesan, R., T. Gnanasekaran, R.S. Srinivasa (2006), "Diffusivity, Activity and Solubility of Oxygen in Liquid Lead and Lead-bismuth Eutectic Alloy by Electrochemical Methods", *Journal of Nuclear Materials*, Vol. 349, pp. 133-149.

Ghetta V.; Gamaoun F.; Fouletier J.; Hénault M.; A. Lemoulec (2001), "Experimental setup for steel corrosion characterization in lead bath", *Journal of Nuclear Materials*, Vol. 296, pp 295-300.

Ghetta, V., J. Fouletier, M. Henault, A. Le Moulec (2002), "Control and Monitoring of Oxygen Content in Molten Metals, Application to Lead and Lead-bismuth Melts", *Journal de Physique IV*, France 12, Pr8, 123-140.

Ghetta, V., A. Maître, J-C. Gachon (2004), "Thermodynamic and Corrosion Studies Related to Liquid PbBi", *Proceedings of the 5th MEGAPIE Technical Review Meeting*, Nantes, France, 24-26 May.

Glasbrenner, H., F. Gröschel (2004a), "Bending Test on T91 Steel in Pb-Bi Eutectic, Bi and Pb-Li Eutectic", *Journal of Nuclear Materials*, Vol. 335, pp. 239-243.

Glasbrenner, H., J. Eikenberg, F. Gröschel, L. Zanini (2004b), "Polonium Formation in Pb-55.5Bi Under Proton Irradiation", *Journal of Nuclear Materials*, Vol. 335, pp. 270-274.

Gorynin, V., G.P. Karzov, V.G. Markov, V.S. Lavrukhin, V.A. Yakovlev (1998), "Structural Materials for Power Plants with Heavy Liquid Metal Systems as Coolant", *Proceedings of the Conference of the Heavy Liquid Metal Coolants in Nuclear Technology*, Obninsk, Russian Federation, 5-9 October, pp. 120.

Gromov, B.F., B.A. Shmatko (1996), "Physico-chemical Properties of Lead-bismuth Alloys", *Izvestiya Vischikh Uchebnikh Zavedenii – iyadernii energiya* (Transaction of Higher Educational Institutions – Nuclear Energy), No. 4, pp. 35-41 (in Russian).

Gromov, B.F., B.A. Shmatko (1997), Izvestiya Vischikh Uchebnikh Zavedenii – iyadernii energiya (Transaction of Higher Educational Institutions – Nuclear Energy), No. 6, pp. 14-18 (in Russian).

Gromov, B.F., Y.I. Orlov, P.N. Martynov, V.A. Gulevskiy (1998), "The Problems of Technology of the Heavy Liquid Metal Coolants (Lead-bismuth, Lead)", *Proceedings of the Conference of the Heavy Liquid Metal Coolants in Nuclear Technology*, Obninsk, Russian Federation, 5-9 October, pp. 87-100.

Gulevskiy, V.A., P.N. Martynov, Yu.I. Orlov (1998), "Application of Hydrogen/Water Vapor Mixtures in Heavy Coolant Technology", *Proceedings of the Conference of the Heavy Liquid Metal Coolants in Nuclear Technology*, Obninsk, Russian Federation, 5-9 October, pp. 668-674.

Gulevskiy, V.A., P.N. Martynov, Yu.I. Orlov, Y.A. Teplyakov, M.E. Chernov (2003), "Water and Hydrogen in Heavy Metal Coolant Technology", *Proceedings of the Fast Neutrons Reactors Conference*, Obninsk, Russian Federation, 8-12 Dec. (in Russian).

Hugon, M., V.P. Bahtnagar, S. Casalta, M. Raynal, S. Webster (2005), "Euratom R&D Programmes on the Back-end of the Fuel Cycle", *Revue générale du nucléaire (RGN)*, No.2, March-April.

HSC Chemistry for Windows Version 4.1, Chemical reaction and equilibrium software, Outokumpu.

JANAF Thermochemical Tables.

IP-EUROTRANS (2004), 6th EURATOM Framework Programme, No. FI6W-CT-2004-516520.

Ivanov, K.D., O.D. Lavrova, P.N. Martynov, S.V. Salayev (2003a), "Impurities in Lead and Lead-bismuth Coolants", *Proceedings of the Fast Neutrons Reactors Conference*, Obninsk, Russian Federation, 8-12 Dec. (in Russian).

Ivanov, K.D., P.N. Martynov, Yu.I. Orlov (2003b), "Pb-Bi Coolant Technology on NPP of Generation I and II", *Proceedings of the Fast Neutrons Reactors Conference*, Obninsk, Russian Federation, 8-12 Dec. (in Russian).

Jacob, K.T., W.W. Shim (1981), "Gibbs Energy of Formation of Lead Zirconate", *Journal of the American Ceramic Society*, Vol. 64, No. 10.

Kawahara, H., S. Ichige, K. Isozaki, S. Nakai (2004), "Replacement of Secondary Heat Transport System Components in the Experimental Fast Reactor JOYO", *Proceedings of ICONE 12*, Arlington, Virginia, USA.

Khorosanov, G.L., A.P. Ivanov, A.I. Blokhin (2002), "Polonium Issue in Fast Reactor Lead Coolants and One of the Ways of its Solution", *Proceedings of ICONE 10*, No. 22330, Arlington, Virginia, USA.

Konys, J., H. Muscher, Z. Voß, O. Wedemeyer (2001), "Development of Oxygen Meters for the Use in Lead-bismuth", *Journal of Nuclear Materials*, Vol. 296, pp. 289-294.

Konys, J., H. Muscher, Z. Voß, O. Wedemeyer (2004), "Oxygen Measurements in Stagnant Lead-bismuth Eutectic Using Electrochemical Sensors", *Journal of Nuclear Materials*, Vol. 335, pp. 249-253.

Korotkov, V.V., K.D. Ivanov, S.V. Salayev (2003), "The Results of the Experimental Investigations Using IPPE Test Facilities in Support of the Technological Regimes of Maintaining the Lead Coolant Quality and the Purity of Self Contained BOR-60 Reactor Channel", *Proceedings of the Fast Neutrons Reactors Conference*, Obninsk, Russian Federation, 8-12 Dec. (in Russian).

Lacressonniere, C. (2003), *Méthode de séparation des isotopes du polonium 208, 209 et 210*, CEA Technical Note DEN/DTN/STR/LCEP 03/032.

Lefhalm, C.H., J.U. Knebel, K.J. Mack (2001), "Kinetics of Gas Phase Oxygen Control System (OCS) for Stagnant and Flowing Pb-Bi Systems", *Journal of Nuclear Materials*, Vol. 296, pp. 301-304.

Loewen, E.P, A.T. Tokuhiro (2003), "Status of Research and Development of the Lead Alloys Cooled Fast Reactor", *Journal of Nuclear Science and Technology*, Vol. 40, No. 8, pp. 614-627.

Li, N. (2002), "Active Control of Oxygen in Molten Lead Bismuth Eutectic Systems to Prevent Steel Corrosion and Coolant Contamination", *Journal of Nuclear Materials*, Vol. 300, pp. 73-81.

Li, N. (2003), in *Advanced Fuel Cycle Initiative*, Quarterly Report, Vol. 1, Jan.-Mar. 2003, Sand2003-2060P.

Li, N. (2004), personal notes.

Martinelli, L., F. Balbaud-Celerier, D. Bosonnet, A. Terlain, G. Santarini, S. Delpech, G. Picard (2005), "High Temperature Oxidation of Fe-9Cr Steel in Stagnant Liquid Lead-bismuth", *Proceedings of the EUROCOOR Conference*, Lisbon, Portugal, 4-8 September.

Martynov, P.N., Y.I. Orlov (1998), "Slagging Processes in Lead Bismuth Loop. Prevention and Elimination of Critical Situations", *Proceedings of the Conference of the Heavy Liquid Metal Coolants in Nuclear Technology*, Obninsk, Russian Federation, 5-9 October, pp. 565-576.

Martynov, P.N., A.V. Gulevich, Y.I. Orlov, V.A. Gulevsky (2005), "Water and Hydrogen in Heavy Liquid Metal Coolant Technology", *Progress in Nuclear Energy*, Vol. 47, No. 1-4, pp. 604-615.

Martynov, P.N., K.D. Ivanov (1998), *Properties of Lead-bismuth Coolant and Perspectives of Non-electric Applications of Lead-bismuth Reactor*, TECDOC 1056, pp. 177-184.

Martynov, P.N., R.S. Askhadullin, N.S. Grachyov, V.A. Gulevskiy, K.D. Ivanov, Yu.I. Orlov, I.V. Yagodkin (2003), "Lead-bismuth and Lead Coolants in New Technologies of Reprocessing of Liquids and Gases", *Proceedings of the Fast Neutrons Reactors Conference*, Obninsk, Russian Federation, 8-12 Dec. (in Russian).

Mueller, G., G. Schumacher, F. Zimmermann (2000), "Investigation on Oxygen Controlled Liquid Lead Corrosion of Surface Treated Steels", *Journal of Nuclear Materials*, Vol. 278, pp. 85-95.

Mueller, G., A. Heinzel, G. Schumacher, A. Weisenburger (2003), "Control of Oxygen Concentration in Liquid Lead and Lead-bismuth", *Journal of Nuclear Materials*, Vol. 321, pp. 256-262.

Muscher, H., J. Konys, Z. Voß; O. Wedemeyer (2001), *Measurement of Oxygen Activity in Lead Bismuth Eutectic by Means of the EMF Method*, FZKA Report 6690, January 2001.

Obara, T., T. Miura, Y. Fujita, Y. Ando, H. Sekimoto (2003), "Preliminary Study of the Removal of Polonium Contamination by Neutron-irradiated Lead-bismuth Eutectic", *Annals of Nuclear Energy*, Vol. 30, pp. 497-502.

Orlov, Y.I., A.D. Efanov, P.N. Martynov, V.A. Gulevsky, A.K. Papovyants, Y.D. Levchenko (2005), "Hydrodynamic Problems of Heavy Liquid Metal Coolant Technology in Loop-type and Monoblock-type Reactor Installations", *Proceedings of the 11th International Topical Meeting on Nuclear Reactor Thermal-hydraulics (NURETH-11)*, Paper No. 220, Avignon, France, 2-6 October.

Pankratov, D., I. Sviatoslav, D. Ridikas, A. Letourneau (2003), "Estimation of ^{210}Po Losses from the Solid ^{209}Bi Irradiated in a Thermal Neutron Flux", *Annals of Nuclear Energy*, Vol. 30, pp. 785-791.

Papovyants, A.K., P.N. Martynov, Y.I. Orlov, Y.D. Boltoev (1998), "Purifying Lead-bismuth Coolant from Solid Impurities by Filtration", *Proceedings of the Conference of the Heavy Liquid Metal Coolants in Nuclear Technology*, Obninsk, Russian Federation, 5-9 October, pp. 675-682 (in Russian).

Perry, R.H. (1997), *Perry's Chemical Engineers' Handbook*, MacGraw-Hill, 7th edition.

Petrovich, C. (2002), *Evaluation of Spallation Products in Lead Bismuth Cooling Systems of ADS-DF*, TECLA Deliverable No. 5, ENEA Technical Note FIS-P130-001, 12 December.

Provorov, A.A., P.N. Martynov, M.E. Chernov, V.A. Gulevskiy, Y.A. Teplyakov (2003), "Methods and Device for Indication of Passivation Films on the Surface of Structural Materials in Heavy Liquid Metal Coolants", *Proceedings of the Fast Neutrons Reactors Conference*, Obninsk, Russian Federation, 8-12 December (in Russian).

Ricapito, I., C. Fazio, G. Benamati (2002), "Preliminaries Studies on PbO Reduction in Liquid LBE by Flowing Hydrogen", *Journal of Nuclear Materials*, Vol. 301, pp. 60-63.

Salayev, S.V., P.N. Martynov, K.D. Ivanov, O.V. Lavrova (2003), "Estimation of the Diffusion Output of Metallic Alloying Elements from the Structural Steels to the Exposure with Heavy Liquid Metal Coolants", *Proceedings of the Fast Neutrons Reactors Conference*, Obninsk, Russian Federation, 8-12 December (in Russian).

Shmatko, B.A., A.E. Rusanov (2000), "Oxide Protection of Materials in Melts of Lead and Bismuth", *Materials Science*, Vol. 36, No. 5, pp. 689-700.

Simakov, A.A., P.N. Martynov, R.S. Askhadullin, V.N. Leonov, V.S. Tsykunov, G.V. Gulevskiy, A.I. Chaban (2003), "Development and Experimental Operations of Mass-exchange Apparatuses for Guaranteeing the Assigned Oxygen Regime in the Heavy Liquid Metal Coolant", *Proceedings of the Fast Neutrons Reactors Conference*, Obninsk, Russian Federation, 8-12 December (in Russian).

Subbarao, E.C. (1980), *Solid Electrolyte and Their Applications*, Plenum Press.

Takahashi, M., H. Sekimoto, *et al*. (2002), "Experimental Studies on Flow Technology and Steel Corrosion of Lead-bismuth", *Proceedings of ICONE 10*, No. 22226, Arlington, Virginia, USA.

Takahashi, M., S. Uchida, H. Osada, Y. Kasahara, K. Matsuzawa, N. Sawa, Y. Yamada, K. Kurome, K. Hata (2003), "Design of Pb-Bi Cooled Direct Contact Boiling Water Small Fast Reactor (PBWFR)", *Proceedings of the Fast Neutrons Reactors Conference*, Obninsk, Russian Federation, 8-12 December (in Russian).

TECDOC-687 (1993), *Fission and Corrosion Product Behaviour in Liquid Metal Fast Breeder Reactors (LMFBRs)*, IAEA.

TECDOC-1056 (1998), *Nuclear Heat Applications: Design Aspects and Operating Experience*, IAEA.

TECDOC-1289 (2002), *Comparative Assessment of Thermophysical and Thermohydraulic Characteristics of Lead, Lead-bismuth, and Sodium Coolants for Fast Reactors*, IAEA.

TECDOC-1348 (2003), *Power Reactors and Sub-critical Blanket Systems with Lead and Lead-bismuth as Coolant and/or Target Material*, IAEA.

TECLA (TECnologies for Lead Alloys) (2000), 5th EURATOM Framework Programme, No. FIKW-CT-2000-00092.

Toshinsky, G.I., *et al.* (2000), "Multipurpose Reactor Module SVBR-75/100", *Proceedings of ICONE 8*, n°8072, Baltimore, USA, 2-6 April.

Ulyanov, V.V., P.N. Martynov, Yu.I. Orlov, V.A. Gulevskiy, Y.A. Teplyakov (2003), "Investigations for the Hydrogen Cleaning Technology of Lead and Lead-bismuth Coolants of Nuclear Tank Facilities", *Proceedings of the Fast Neutrons Reactors Conference*, Obninsk, Russian Federation, 8-12 December (in Russian).

Warin, D. (2002), "Transmutation Studies in Europe", *Revue générale du nucléaire (RGN)*, No. 4, August-September.

Zhang, J., N. Li (2004), "Corrosion/Precipitation in Non-isothermal and Multi-modular LBE Loop Systems", *Journal of Nuclear Materials*, Vol. 326, pp. 201-210.

Zrodnikov, A.V., A.D. Efanov, Y.I. Orlov, P.N. Martynov, V.A. Gulevskiy, V.M. Troyanov, A.E. Rusanov (2003), "Heavy Liquid Metal Coolants Technology (Pb-Bi and Pb)", *3rd International Workshop on Materials for Hybrid Reactors and Related Technologies*, Rome, October 2003.